2021

Interleukin 33 triggers early eosinophil-dependent events leading to metaplasia in a chronic model of gastritis-prone mice

Carlo De Salvo

Jason C. Mills

et al

Interleukin 33 Triggers Early Eosinophil-Dependent Events Leading to Metaplasia in a Chronic Model of Gastritis-Prone Mice

Carlo De Salvo,[1] Luca Pastorelli,[1,2,3] Christine P. Petersen,[4] Ludovica F. Buttò,[5] Kristine-Ann Buela,[1] Sara Omenetti,[1] Silviu A. Locovei,[1,5] Shuvra Ray,[1] Hannah R. Friedman,[1] Jacob Duijser,[1] Wei Xin,[1] Abdullah Osme,[1] Fabio Cominelli,[5] Ganapati H. Mahabeleshwar,[1] Jason C. Mills,[6] James R. Goldenring,[4] and Theresa T. Pizarro[1]

[1]Department of Pathology, Case Western Reserve University School of Medicine, Cleveland, Ohio; [2]Gastroenterology Unit, Istituto di Ricovero e Cura a Carattere Scientifico Policlinico San Donato, San Donato Milanese, Milan, Italy; [3]Department of Biomedical Sciences for Health, University of Milan, Milan, Italy; [4]Department of Surgery and the Epithelial Biology Center, Vanderbilt University, Nashville, Tennessee; [5]Division of Gastroenterology & Liver Disease, Department Medicine, Case Western Reserve University School of Medicine, Cleveland, Ohio; and [6]Gastroenterology Division, Department of Medicine, Washington University in St. Louis School of Medicine, St Louis, Missouri

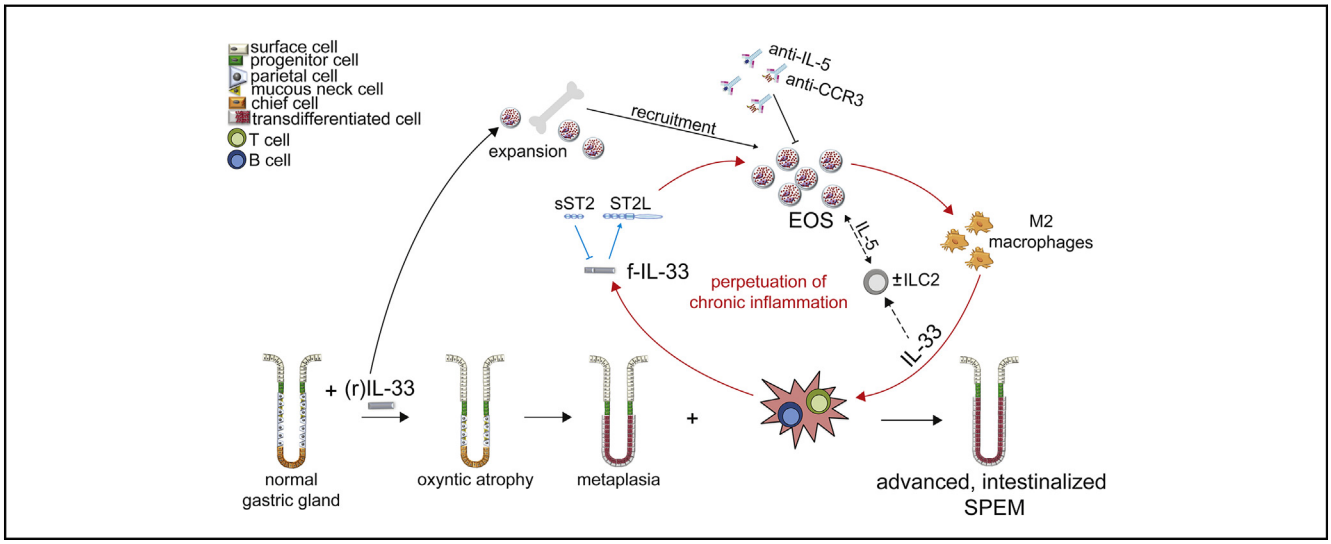

BACKGROUND & AIMS: Interleukin (IL)33/IL1F11 is an important mediator for the development of type 2 T-helper cell (Th2)–driven inflammatory disorders and has also been implicated in the pathogenesis of gastrointestinal (GI)-related cancers, including gastric carcinoma. We therefore sought to mechanistically determine IL33's potential role as a critical factor linking chronic inflammation and gastric carcinogenesis using gastritis-prone SAMP1/YitFc (SAMP) mice. **METHODS:** SAMP and (parental control) AKR mice were assessed for baseline gastritis and progression to metaplasia. Expression/localization of IL33 and its receptor, ST2/IL1R4, were characterized in corpus tissues, and activation and neutralization studies were both performed targeting the IL33/ST2 axis. Dissection of immune pathways leading to metaplasia was evaluated, including eosinophil depletion studies using anti-IL5/anti-CCR3 treatment. **RESULTS:** Progressive gastritis and, ultimately, intestinalized spasmolytic polypeptide-expressing metaplasia (SPEM) was detected in SAMP stomachs, which was absent in AKR but could be moderately induced with exogenous, recombinant IL33. Robust peripheral (bone marrow) expansion of eosinophils and local recruitment of both eosinophils and IL33-expressing M2 macrophages into corpus tissues were evident in SAMP. Interestingly, IL33 blockade did not affect bone marrow-derived expansion and local infiltration of eosinophils, but markedly decreased M2 macrophages and SPEM features, while eosinophil depletion caused a significant reduction in both local IL33-producing M2 macrophages and SPEM in SAMP. **CONCLUSIONS:** IL33 promotes metaplasia and the sequelae of eosinophil-dependent downstream infiltration of IL33-producing M2 macrophages leading to intestinalized SPEM in SAMP, suggesting that IL33 represents a critical link between chronic gastritis and intestinalizing metaplasia that may serve as a potential therapeutic target for preneoplastic conditions of the GI tract.

Keywords: IL-33/ST2 Axis; M2 Macrophages; SPEM/Intestinalized SPEM; Gastric Cancer.

WHAT YOU NEED TO KNOW

BACKGROUND AND CONTEXT

The link between chronic, non-resolving inflammation and cancer is well established, with inflammation-associated cancers among the most highly represented and frequently-occurring neoplasias worldwide. Investigation over the last several years has focused on determining critical pathways involved in this process, with a number of candidate molecules identified, including members of the interleukin-1 (IL-1) family that are particularly important in cancers of the GI tract.

NEW FINDINGS

IL-33 (or IL-1F11), a member of the IL-1 family of cytokines, serves as an important mediator linking chronic inflammation and metaplasia by inducing the expansion and recruitment of activated eosinophils leading to advanced, intestinalized SPEM in gastritis-prone SAMP1/YitFc (SAMP) mice.

LIMITATIONS

Further studies are warranted to determine the precise inciting factors of increased IL-33 leading to intestinalized SPEM in SAMP mice, as well as in patients with gastric cancer.

IMPACT

The present manuscript contributes to a better understanding of potential mechanism(s) that promote the inflammation-metaplasia-dysplasia-carcinoma sequelae that can apply to several GI-related cancers.

The link between chronic inflammation and cancer is well established, with inflammation-associated cancers among the most highly represented and frequently occurring neoplasias worldwide.[1,2] Investigation over the last several years has focused on determining critical pathways involved in this process, with a number of candidate molecules identified, including members of the interleukin (IL) 1 family that are particularly important in gastrointestinal (GI)-related cancers.[3,4] Of these, IL33 plays a prominent role in intestinal tumorigenesis, both in mouse models of adenomatous polyposis (ie, Apc^{Min} strain) and inflammation-associated colorectal cancer, as well as in patients with colorectal adenocarcinoma.[5–7]

Less is known regarding the contribution of IL33 to the development of upper GI cancers, including gastric adenomas, which generally occur as a consequence of chronic gastritis after prolonged *Helicobacter* (*H*) *pylori* infection or as a result of autoimmune gastritis.[8] As such, while IL33 clearly plays a paramount role in both inflammation and cancer, a definitive link between IL33-dependent inflammation and carcinogenesis in the GI tract has yet to be determined.

IL33/interleukin 1 family member 11 (IL1F11) is widely distributed throughout various organ systems, primarily in nonhematopoietic cells, but also in cells of hematopoietic origin, particularly in restricted populations of professional antigen-presenting cells such as macrophages.[9,10] IL33 was initially associated with type 2 T-helper cell (Th2) immunity, based on expression of its cell-bound receptor, ST2L/IL1R4, on polarized Th2 lymphocytes[9] and more recently, on group 2 innate lymphoid cells (ILC2s),[11] and its ability to effectively induce M1, but more commonly M2 macrophage differentiation.[12] Importantly, IL33 also potently activates and induces eosinophil infiltration into mucosal organs that interface with the external environment, such as the GI and respiratory tracts.[9,13,14]

Relevant to the present study, prior reports associate IL33 with poor prognosis in gastric cancer patients,[15] and in vitro experiments suggest that IL33 confers chemoresistance[16] and increased invasiveness[17] of gastric cancer cells. Recently, IL33-dependent activation of mast cells was shown to promote tumor angiogenesis and growth that, in combination with tumor-associated macrophages, positively correlates with decreased survival of gastric cancer patients.[18] As such, although evolving, the precise role of IL33 in gastric cancer has not yet been fully elucidated; specifically, how IL33 mechanistically exerts the aforementioned effects and whether IL33 contributes to the development of preneoplastic states ultimately leading to gastric cancer.

In fact, chronic inflammatory conditions of the stomach often result in reactive modifications of the mucosa, including atrophy of mature acid-secreting cells as new metaplastic lineages arise. Such metaplastic changes in epithelial cells increase the risk of developing dysplasia and gastric cancer.[19–21] The initial metaplasia that arises, concomitant with acid-secreting parietal cell atrophy, is defined by the existence of antral-like mucous cells within the body (corpus) of the stomach and is known as spasmolytic polypeptide-expressing metaplasia (SPEM), or pseudopyloric metaplasia. SPEM[22] is thought to arise from reprogramming of mature chief cells after parietal cell loss[23–25] and is thus named by the induced expression of spasmolytic polypeptide (ie, trefoil factor 2 [TFF2]), in metaplastic cells.[23,26–28]

In addition to SPEM, the stomach can undergo intestinal metaplasia,[19] which is confirmed by the presence of intestinal lineages such as mucus-secreting goblet cells. Chronic inflammation can promote the progression of metaplastic mucosa to a more proliferative phenotype that is at risk for progression to dysplasia and cancer.[29] Experimentally, SPEM can be chemically induced by L635, a parietal cell-specific protonophore that generates a cascade of events leading to oxyntic atrophy, infiltration of activated M2-

Abbreviations used in this paper: **Apc, adenomatous polyposis coli; BM, bone marrow; BrdU, 5-bromo-2-deoxyuridine; CCR3, C-C motif chemokine receptor 3; CD, cluster of differentiation; Clu, clusterin; Fc, fragment crystallizable; fIL33, full-length interleukin 33; GIF, gastric intrinsic factor; GSII, *Griffonia simplicifolia* lectin II; *H pylori*, *Helicobacter pylori*; IL, interleukin; ILC2, type 2 innate lymphoid cells; Il1rl1, interleukin-1 receptor-like 1; LP, lamina propria; MBP, major basic protein; PAS, periodic acid–Schiff; PFA, paraformaldehyde; qPCR, quantitative polymerase chain reaction; rIL33, recombinant interleukin 33; SAMP, SAMP1/YitFc; SPEM, spasmolytic polypeptide-expressing metaplasia; TFF1/2, trefoil factor 1/2.**

Most current article

0016-5085/$36.00
https://doi.org/10.1053/j.gastro.2020.09.040

polarized macrophages, and SPEM that can develop intestinal characteristics in mice.[30] When this model is used, IL33 promotes IL13-dependent M2 polarization of recruited macrophages and the development of SPEM.[31]

In the present study, we evaluate a murine model, SAMP1/YitFc (SAMP) strain,[32] that spontaneously develops chronic gastric inflammation to uncover potential IL33-dependent mechanism(s) leading to and downstream of parietal cell loss and chief cell transdifferentiation that can result in SPEM and an even more proliferative, intestinalized SPEM. We show that:

1. gastritis-prone SAMP mice progressively develop metaplasia leading to advanced SPEM-like features;
2. exogenous recombinant (r)IL33 administration induces moderate metaplasia and M2 macrophage infiltration in stomachs of healthy (AKR) mice, and under chronic inflammatory conditions, exacerbates and advances metaplasia-acquiring intestinal characteristics in SAMP;
3. neutralization of IL33 in SAMP with established disease dampens gastritis and progression of metaplasia/SPEM;
4. IL33 induces potent peripheral eosinophil expansion and subsequent recruitment into stomachs of treated mice; and
5. eosinophil depletion markedly diminishes M2 macrophage infiltration and SPEM-like features in SAMP.

Together, our data suggest that IL33 plays a central role in the early events leading to SPEM and that during chronic inflammation, or perhaps under other predisposing conditions that promote lack of immune tolerance, or both, IL33-dependent eosinophil activation and migration are essential for this process to occur. As such, targeting the IL33/ST2 axis for therapeutic purposes may be beneficial for the treatment or prevention, or both, of preneoplastic states leading to gastric cancer.

Materials and Methods

Mice

Mice were provided through core services supported by the Animal and Mouse Models Cores of National Institutes of Health National Institute of Diabetes and Digestive and Kidney Diseases P01 DK091222 and P30 DK097948, respectively. SAMPx*Il33*$^{-/-}$ mice were developed by backcrossing male C57BL/6J (B6) mice homozygous for a null allele of *Il33* (*Il33*$^{-/-}$)[5,33] with female SAMP for 10 generations and validated by microsatellite analysis comparing SAMP- vs B6-specific markers. Breeding of F_1N_{10} heterozygous offspring generated SAMP homozygous *Il33*$^{-/-}$, heterozygous, and wild-type controls, identified by polymerase chain reaction (PCR).[5,33] Mice were maintained as previously described,[34] with all procedures approved by the Case Western Reserve University Institutional Animal Care and Use Committee.

Tissue Harvest and Histologic/Spasmolytic Polypeptide-Expressing Metaplasia Assessment

Mice were euthanized and whole stomachs removed and opened along the greater curvature. Forestomach and antrum were excised, and the corpus was dissected along the longitudinal plane, with 1 strip each placed in RNA*later* (Ambion, Thermo Fisher Scientific, Waltham, MA) or radioimmunoprecipitation buffer (Pierce Biotechnology, Rockford, IL) and maintained at −20°C until later RNA and protein extraction, respectively. The remaining tissue strip was submerged in Bouin's Fixative Solution (Ricca Chemical Company, Arlington, TX), 4% paraformaldehyde (PFA) (ChemCruz, Santa Cruz Biochemicals, Dallas, TX), or methacarn. Bouin's/PFA- and methacarn-fixed tissues were rinsed in 70% ethanol after 24 hours or 20 minutes, respectively, processed, paraffin-embedded, and sectioned at 3 to 4 μm. Specimens were stained with H&E or Alcian blue/periodic acid–Schiff (PAS) with optional hematoxylin 7221 (Thermo Scientific Richard-Allan Scientific, Kalamazoo, MI).

Samples were evaluated by trained GI pathologists (W.X., A.O.) in a blinded fashion for gastritis/epithelial alterations and SPEM/intestinalized SPEM as previously described.[30,32] SPEM was scored by calculating the percentage of cross-sectional involvement, defined by oxyntic atrophy with loss of parietal cells and replacement of gastric glands with mucous cell lineages staining positive for PAS/Alcian blue.

In Vivo Studies

Experiments were conducted in a blinded manner, with mice randomized to different interventions using progressive numeric labeling, the code only known to animal caretakers and revealed at end of each experiment. Scientific rigor, data reproducibility, and biological variables were followed, based on recently published guidelines.[35] SAMP and sex- and age-matched AKR mice were evaluated for baseline gastritis and progression to SPEM/intestinalized SPEM.[30,32] For exogenous IL33 experiments, 8- to-12-week-old mice were injected intraperitoneally with rIL33 (33 μg/kg) (Enzo Life Sciences, Farmingdale, NY) or Hank's buffered salt solution (vehicle), daily for 1 week. IL33 neutralization was achieved using a fusion protein (5 mg/kg, intraperitoneally twice weekly for 4 weeks) consisting of the extracellular domain of mouse soluble (s)ST2 fused to IgG1-Fc (sSt2-Fc); controls were similarly administered IgG1-Fc (Dirk E. Smith, Amgen, Inc., Seattle, WA). Eosinophil depletion was performed using monoclonal antibodies against IL5 and C-C motif chemokine receptor 3 (CCR3) and controls treated with an isotype IgG.[34]

Quantitative Reverse-Transcription Polymerase Chain Reaction and Western Blots

Total RNA was isolated, reverse-transcribed, and quantitative polymerase chain reaction (qPCR) performed as previously described,[34] using specific target gene primers (Supplementary Table 1) normalized to β-actin or *36B4* and reported as relative fold-difference among groups, with baseline/controls set arbitrarily at 1. Total protein extracts from the corpus were prepared and Western blotting was performed.[10,33]

Staining With 5-Bromo-2-Deoxyuridine and Immunohistochemistry

Mice were injected with 5-bromo-2-deoxyuridine (BrdU) labeling agent (Invitrogen, Carlsbad, CA) 2 hours before euthanization. Gastric tissues were harvested, fixed in 4% PFA, and stained following the manufacturer's instructions (BrdU

Staining Kit; Invitrogen). Immunohistochemistry was performed using a polyclonal goat anti-mouse IL33 IgG (R&D Systems, Minneapolis, MN), biotinylated *Dolichos biflorus* agglutinin (DBA, Vector Laboratories, Burlingame, CA), or a monoclonal rat anti-mouse major basic protein (MBP) IgG (clone MT-14.7) (James J. Lee, Mayo Clinic, Scottsdale, AZ), with negative controls prepared under identical conditions in the absence of respective primary antibodies.[34]

Parietal cell/eosinophil counts were calculated by average intact, nucleated cells positive for DBA/MBP in 10 randomly selected high-power fields.[34] Immunofluorescence for confocal imaging was performed to detect *Griffonia simplicifolia* II (GSII), cluster of differentiation (CD) 44v, clusterin (Clu), CD163, IL33, gastric intrinsic factor (GIF), and imaged/analyzed by the Vanderbilt Digital Histology Shared Resource.[31]

Flow Cytometry

Bone marrow (BM) from femurs/tibias was harvested and processed as previously described.[34] Corpus tissues were processed into single-cell suspensions.[31] Then, 2×10^6 cells were stained with LIVE/DEAD Fixable Near-IR Dead Cell Stain (Thermo Fisher Scientific) and specific antibodies to detect eosinophils and M2 macrophages (Supplementary Table 2). Samples were acquired with a BD LSR II flow cytometer and data analyzed with FlowJo Software (both, Becton Dickinson, Franklin Lakes, NJ).[31,34]

Statistical Analyses

Data were analyzed using GraphPad Prism 5 (GraphPad Software, Inc, San Diego, CA). Selection of appropriate statistical tests was based on variance and underlying distribution of data. Global effects between groups were assessed using 1-way analysis of variance with Bonferroni's correction for multiple comparisons. Differences between individual groups were directly compared using the 2-sample unpaired Student's *t* test, and results are expressed as mean ± SEM, unless otherwise indicated, with $P < .05$ considered significant.

Results

Gastritis-Prone SAMP Exhibit Morphologic Features and a Molecular Profile Consistent With Intestinalized Spasmolytic Polypeptide-Expressing Metaplasia

SAMP mice develop chronic, immune-mediated gastritis with increased severity over time.[32] Stomachs from 20-week-old SAMP show remarkable and progressive parietal cell loss compared with age-matched AKR controls, which possess abundant parietal cells (Supplementary Figure 1*A*). The emergence of prominent Alcian blue/PAS-stained hyperplastic mucous neck cells in SAMP highlight the presence of acidic mucins, commonly found in SPEM and adenocarcinoma,[36] but are absent in AKR (Supplementary Figure 1*A*). Older SAMP display intense staining for the mucous marker, GSII lectin, while colocalization with CD44v or Clu, indicative of SPEM, shows more intense Clu expression along the gastric glands compared with AKRs. The presence, albeit subtle, of Cd44v at the base of gastric glands in 20-week-old SAMP is also detected but is virtually absent in the other experimental groups (Supplementary Figure 1*B*).

Molecular profiling of full-thickness corpus shows a striking decrease in the expression of genes associated with oxyntic atrophy and foveolar hyperplasia, including gastric intrinsic factor (*Gif*), adenosine-5'-triphosphatase H^+/K^+ transporting alpha subunit (*Atp4a*), and trefoil factor 1 (*Tff1*), comparing SAMP vs AKR, particularly in older mice (Supplementary Figure 2*A*). During acute oxyntic atrophy, as parietal cells die, chief cells show a rapid decrease in the zymogen granule maturation transcription factor (*Mist1*) and an increase in *Tff2*.[26,37] Although no differences in *Tff2* are detected among experimental groups, *Mist1* is markedly decreased in SAMP vs AKR (Supplementary Figure 2*B*). Furthermore, the SPEM markers, human epididymis protein 4 (*He4*), *Clu*, lysozyme (*Lyz*), and glutathione peroxidase 2 (*Gpx2*),[29,37] are all dramatically increased in SAMP with established disease vs AKR (Supplementary Figure 2*C*). Importantly, markers of more advanced, proliferative lesions (intestinalized SPEM),[29,30] including cystic fibrosis transmembrane conductance regulator (*Cftr*) and deleted in malignant brain tumors protein 1 (*Dmbt1*), are strongly upregulated in 20-week-old SAMP vs AKR, while the early tumor shrinkage variant 5 (*Etv5*) transcription factor is unchanged (Supplementary Figure 2*D*).

Increased Circulating Interleukin 33, With Its Most Bioactive Form Localizing to Gastric M2 Macrophages in SAMP With Advanced Spasmolytic Polypeptide-Expressing Metaplasia

To test the hypothesis that increased and persistent exposure to IL33 may be needed for intestinalized SPEM to occur, we initially measured systemic/circulating IL33, which is substantially increased in SAMP, even before histologically evident gastritis (at 4 weeks) and dramatically rises as disease becomes more severe, compared with IL33 in AKR that remains relatively stable (Supplementary Figure 3). Locally, within nondiseased stomachs of 4-week-old mice, IL33 is primarily found in foveolar epithelium, almost exclusively localized to nuclei (Figure 1*A*). In older mice, AKR retain some epithelial-specific nuclear expression with scant $IL33^+$ cells within the lamina propria (LP), while abundant and diffuse IL33 immunoreactivity is observed in SAMP, also within the LP, as well as at the base of the mucosa (Figure 1*A*).

Evaluation of IL33 isoforms reveals less abundant IL33 in 4-week-old SAMP compared with AKR; however, in older SAMP, only full-length IL33 (fIL33), representing its most bioactive 30-kD form,[38] is prominently expressed, whereas other less bioactive forms[39,40] are present in AKR (Figure 1*B*). In fact, SAMP express mainly fIL33, whereas the 20- to 22-kD cleaved form (cIL33) is virtually undetectable but clearly present in AKR (Figure 1*B*), suggesting increased release of bioactive fIL33 in SAMP with established disease. Surprisingly, *Il33* in SAMP stomachs is decreased compared with AKR (Figure 1*C*), which may be due to high circulating IL33

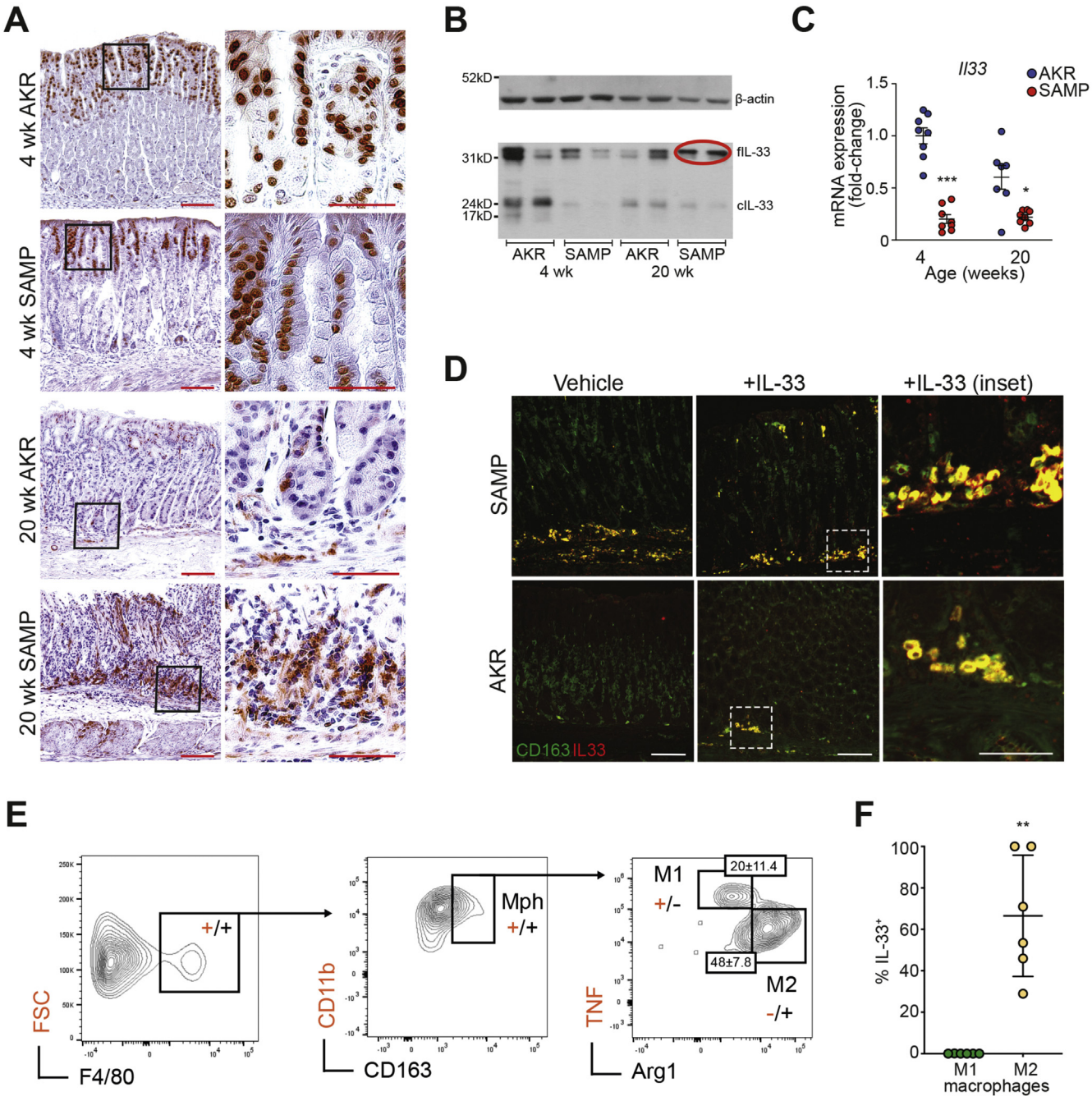

Figure 1. Differential IL-33 localization/expression in corpus of gastritis-prone SAMP vs control AKR. (*A*) Representative immunohistochemistry images localizing IL33 before inflammation (4 weeks old) and during established disease (20 weeks old) in SAMP (N = 8). Original magnification ×10+2.0 and ×40+2.0 (*insets*); *scale bars*: 100 μm and 50 μm (*insets*). (*B*) Representative Western blot differentiating bioactive fIL33 from cIL33 (N = 4). (*C*) *Il33* expressed as fold-change vs age-matched AKR (N = 7–8). mRNA, messenger RNA. **P* < .05, ****P* < .001. (*D*) Immunofluorescent colocalization of IL-33 (*red*) and CD163 (*green*) show abundance of IL-33–producing M2 macrophages (*yellow*), further augmented after rIL33 in AKR (N = 4), and (*E*) confirmed by fluorescence-activated cell sorter (N = 6). (F) frequency of IL-33-expressing M2 vs M1 macrophages (N=6). Original magnification ×20; *scale bars*: 10 μm and 5 μm (*insets*). FSC, forward scatter; TNF, tumor necrosis factor. ***P* < .01.

levels (Supplementary Figure 3) and potential negative feedback mechanism(s) downregulating IL33's bioactivity.

Finally, to identify the cellular source of the considerable yet diffuse IL33 staining within the gastric submucosa of older SAMP (Figure 1*A*), immunofluorescent colocalization studies were performed, revealing abundant, infiltrating IL33-expressing CD163^{+} M2 macrophages that are virtually absent in noninflamed AKR but can be elicited with rIL33 (Figure 1*D*). Phenotypic characterization of SAMP gastric mucosal cells confirm the presence of IL33-producing M2 macrophages (Supplementary Figures 4 and 1*E* and *F*), with

an overall dominant M2 vs M1 profile vs AKR (Supplementary Figure 5).

Exogenous Administration of Interleukin 33 Induces Spasmolytic Polypeptide-Expressing Metaplasia in Normal (AKR) Mice

One of the original observations regarding IL33's bioactivity was its ability to promote epithelial hyperplasia, mainly in goblet cells, within GI and airway mucosae.[9] These findings were confirmed in stomachs of IL33-treated B6 mice, which results in a Th2/signal transducer and activator of transcription 3 (STAT3)-driven gastric pathology.[41] Aside from inducing infiltration of IL33-expressing CD163$^+$ M2 macrophages (Figure 1*D*), acute systemic exposure of IL33 AKR consistently promotes the gross anatomic appearance of thickened gastric mucosal folds that are absent in vehicle-treated mice (Figure 2*A*). Histologic evaluation of these folds reveals striking alterations, including overall hypertrophy of the gastric mucosa, epithelial hyperplasia, as well as oxyntic atrophy, while parietal and chief cells remain relatively intact in vehicle-treated AKR (Figure 2*A*). Interestingly, although exogenous IL33 results in only 25% of AKR displaying significant gastritis, increased epithelial hyperplasia suggests its contribution to inducing mucous neck cell hyperplasia and metaplasia (Figure 2*B*).

The presence of metaplasia is further characterized by prominent proliferation of cells within the gastric glands, demonstrated by a greater number of BrdU$^+$ cells, along the neck and at the base of gastric glands (Figure 2*A*, *right*

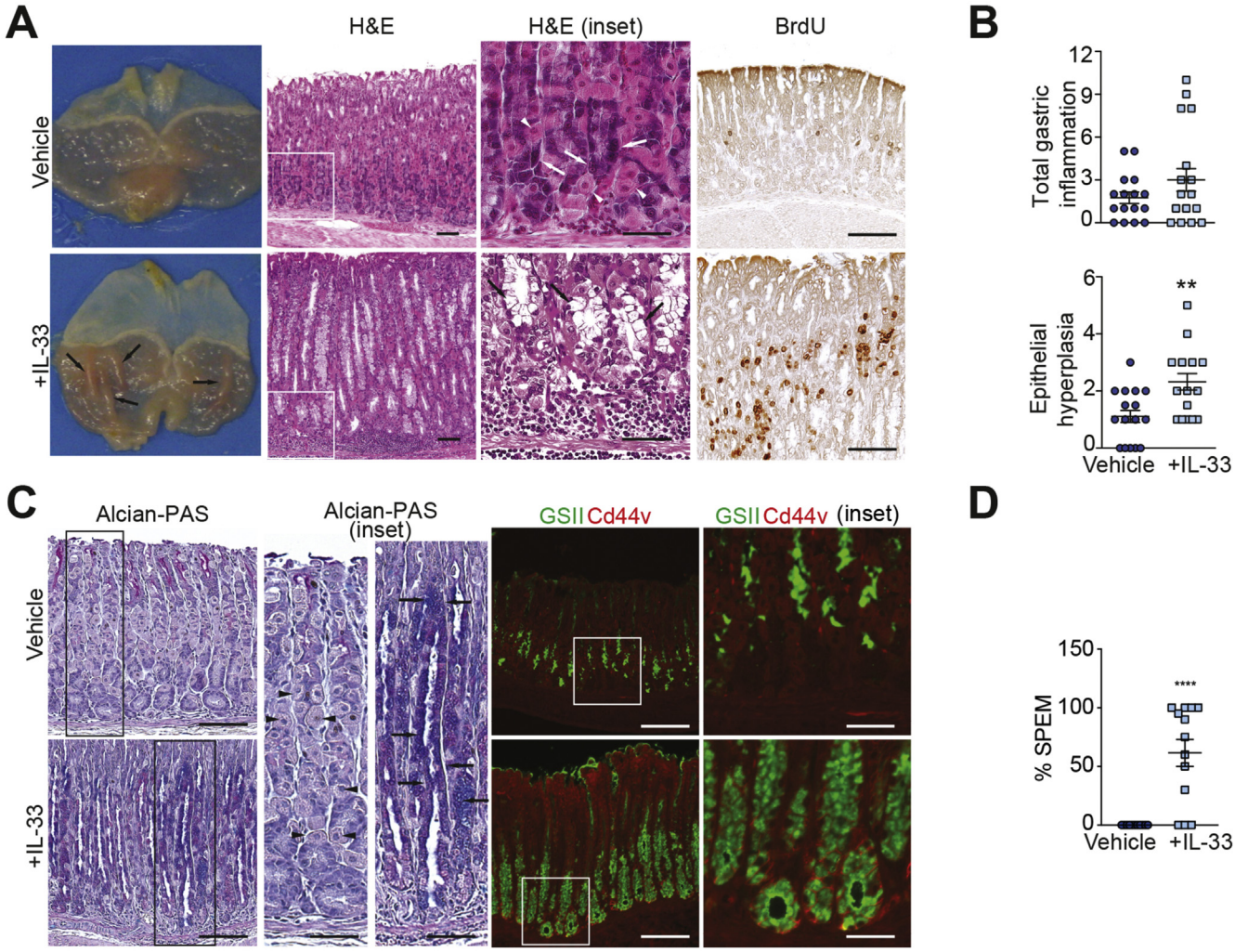

Figure 2. IL33 administration to healthy AKR induces striking gastric mucosal alterations. (*A*) Representative photographs of bisected stomachs, highlighting presence of gastric mucosal folds (*black arrows*), and photomicrographs of corpus displaying parietal cell (*white arrowheads*) atrophy, loss of chief cell (*white arrows*) differentiation, hyperproliferation of mucus-producing cells (*black arrows*), and active proliferation of BrdU$^+$ mucous neck cells after rIL33; original magnification ×10 and ×40 (*insets*); *scale bars*: 100 μm and 50 μm (*insets*). (*B*) Quantitation of gastric inflammation and epithelial hyperplasia. (*C*) Representative photomicrographs show the appearance of acidic mucins by Alcian blue/PAS-staining (*arrows*; parietal cells indicated by *arrowheads*), and increased presence/intensity of GSII lectin (*green*) and CD44v (*red*) after rIL33; original magnification (left-to-right) ×20+1.25, ×40+1.25, ×20, and ×40 (*insets*); *scale bars*: 100 μm and 50 μm (*insets*). (*D*) Semi-quantitative assessment of SPEM (n = 13-16). $^{**}P < .01$, $^{****}P < .0001$.

panels), and Alcian blue/PAS staining, highlighting the appearance of hyperplastic acidic mucin-producing neck cells, comparing IL33- vs vehicle-treated AKRs (Figure 2*C*).

Finally, accumulation of GSII lectin (a surrogate for MUC6 expression) colocalizing with CD44v at the base of glands in treated AKR (Figure 2*C*), indicating chief cells transdifferentiation,[42] also supports the development of IL33-dependent SPEM (Figure 2*D*), but for the most part, in the absence of inflammation.

Consistent with oxyntic atrophy, molecular profiling shows that *Gif* and *Atp4a* are downregulated in corpus tissues from IL33-treated AKR (Figure 3*A*), and while *Tff1* shows a trend toward decreased expression, *Tff2* is strongly upregulated after short-term IL33 exposure (Figure 3*A*), further indicating the occurrence of IL33-induced chief cell transdifferentiation leading to SPEM. Additionally, *He4* and *Clu* are consistently upregulated after rIL33 (Figure 3*B*); however, only *Cftr* is considerably increased for the intestinalized SPEM markers assayed (Figure 3*C*), suggesting that IL33 has a prominent effect on the development of SPEM, but to progress to a more advanced intestinalized phenotype, a longer, more chronic exposure to IL33 may be needed. Interestingly, exogenous IL33 does not affect *Il1rl1* (ST2L), encoding the signaling receptor for IL33, but *Il1rl1* (sST2), encoding soluble ST2, an IL33-specific decoy receptor,[43] is markedly increased and *Il33* is significantly decreased (Figure 3*D*), which is similar to what is observed in SAMP with established disease and may represent a negative feedback response after rIL33.

Blockade of Interleukin 33 Signaling Dampens Spasmolytic Polypeptide-Expressing Metaplasia Progression in SAMP Mice

To test whether IL33 neutralization is effective in dampening or reversing intestinalized SPEM, we administered sST2-Fc to SAMP with established disease. Treatment with sST2-Fc reduces expression of CD44v and does not appear to change GIF compared with vehicle controls but has a significant impact on diminishing the number of IL33-producing $CD163^{+}$ M2 macrophages as well as GSII expression (Figure 4*A*, *right panels*). Histologically, global improvement is evident in regards to epithelial architecture and gland structure, with decreased Alcian blue/PAS-stained cells, indicating diminished production of acidic mucins. A substantially increased census of cells positive for the parietal cell-specific marker, DBA, is also observed, consistent with morphology of parietal cell precursors (Figure 4*A* and *B*), which dramatically arise during restitution from SPEM.[44] Histologic evaluation shows a 57% decrease in epithelial hyperplasia after IL33 blockade (Figure 4*C*), suggesting

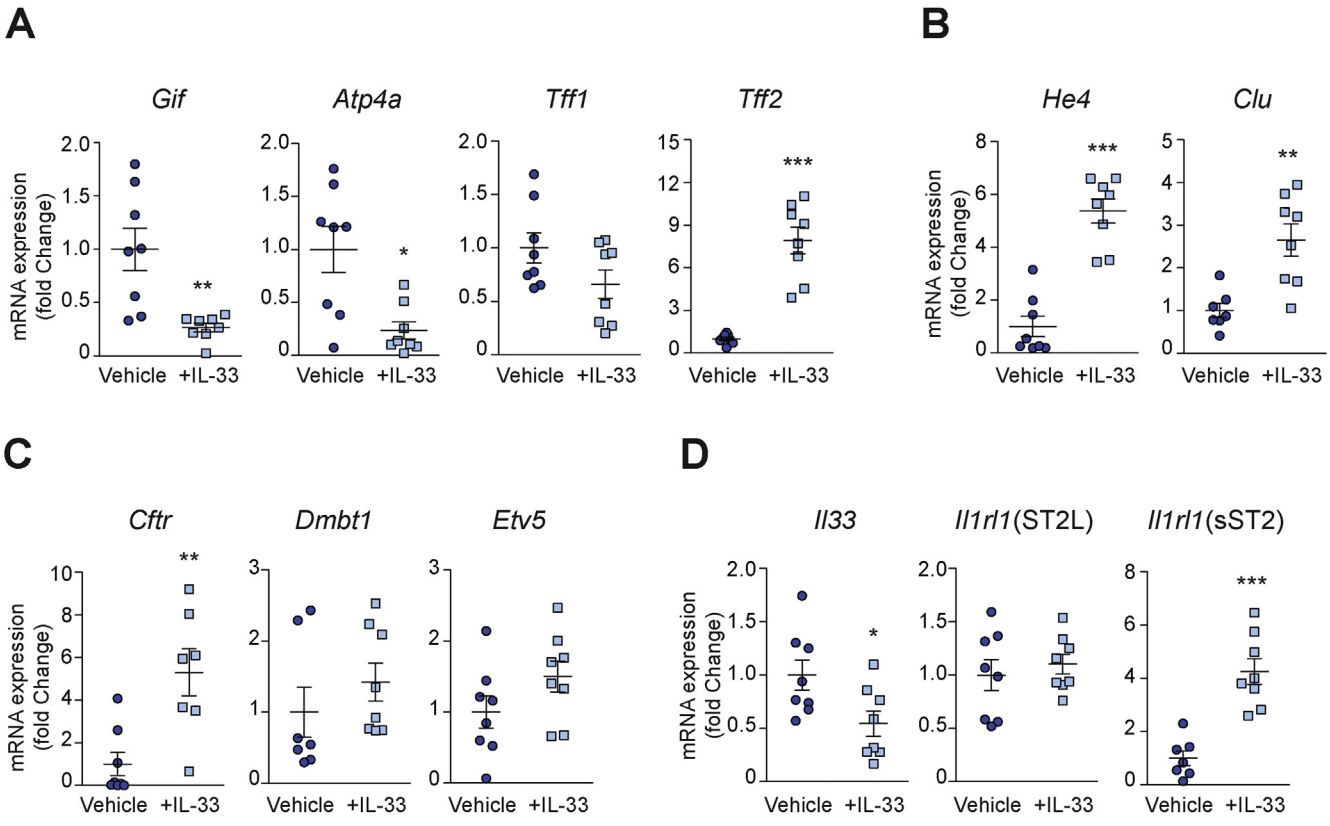

Figure 3. Molecular profiling indicates overt metaplasia in AKR corpus after acute exposure to IL33. Relative transcript levels of (*A*) *Gif*, *Atp4a*, *Tff1*, and *Tff2*, (*B*) *He4* and *Clu*, (*C*) *Cftr*, *Dmbt1*, and *Etv5*, and (*D*) *Il33*, and *Il1rl1* variant 1 (ST2L) and 2 (sST2) after rIL33. Data are expressed as fold-change vs vehicle controls (N = 8). mRNA, messenger RNA. **P* < .05, ***P* < .01, ****P* < .001.

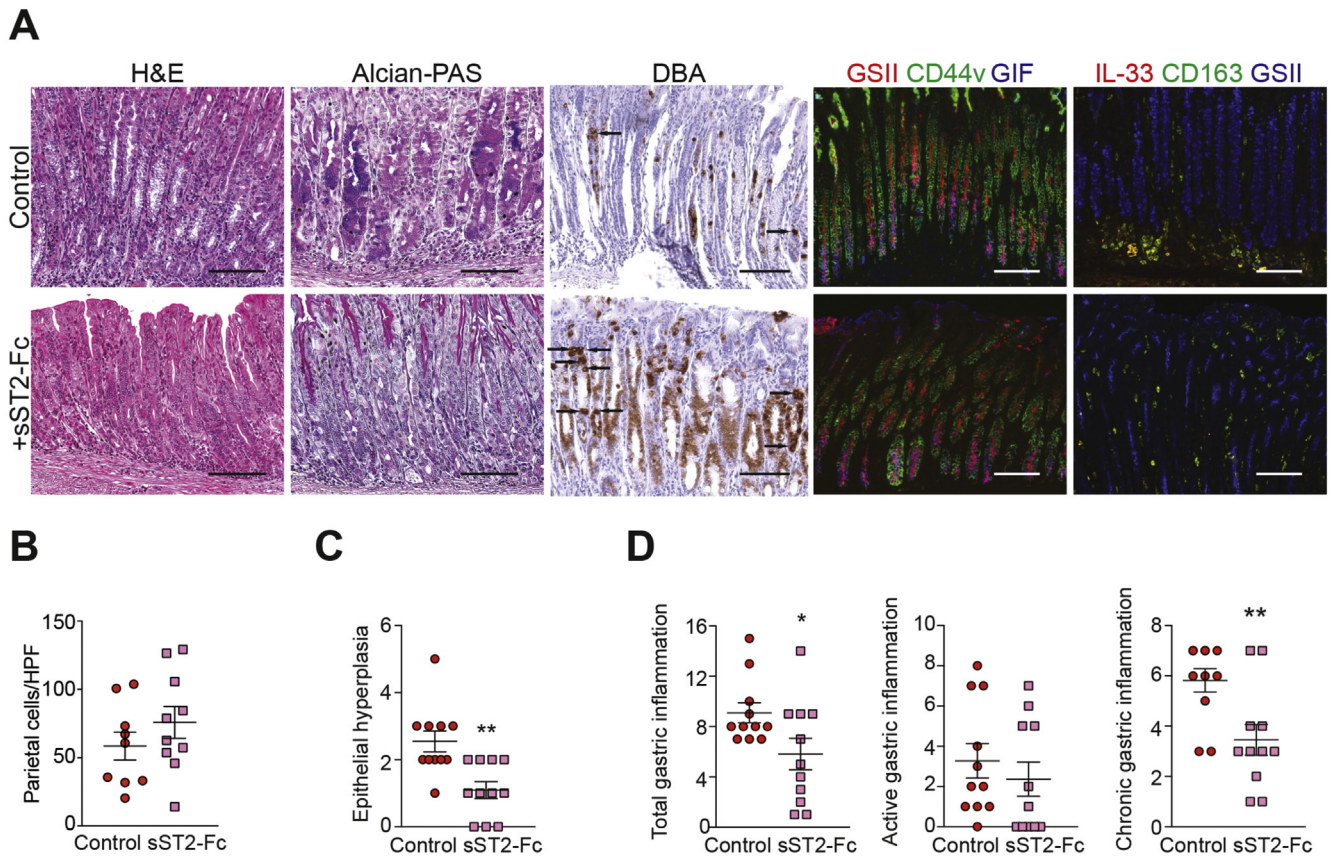

Figure 4. Neutralization of IL33 attenuates chronic gastritis and intestinalized SPEM in SAMP. (*A*) Representative photomicrographs of corpus stained with H&E, Alcian blue/PAS, and DBA after sST2-Fc (*left panels*). Immunofluorescence for GIF (*blue*) remains relatively unchanged, but CD44v (*green*) and GSII-lectin (*red/blue*) are decreased, and IL33 (*red*)/CD163 (*green*) shows marked reduction of IL33-producing M2 macrophages (*yellow*) after sST2-Fc (*right panels*). Original magnification ×20+1.25; scale bars: 100 μm. (*B*) Parietal cell numbers per high-power field (HPF) (*arrows*, panel *A*), (*C*) epithelial hyperplasia, and (*D*) gastric inflammation after sST2-Fc (N = 9–11). *$P < .05$, **$P < .01$.

restorative epithelial processes toward normal homeostasis.

Histology images also show that overall gastric inflammation is visibly decreased after IL33 blockade vs control, confirmed by reduction in total inflammatory scores (Figure 4*D*). Of note, the primary component driving total inflammation downward in sST2-Fc–treated SAMP is chronic inflammation, which decreases by 41%, and not acute inflammation, which remains relatively unchanged between experimental groups (Figure 4*D*).

Peripheral Expansion and Local Recruitment of Eosinophils Are Dramatically Increased in SAMP With Advanced Spasmolytic Polypeptide-Expressing Metaplasia and Rely on Interleukin 33

We previously reported that eosinophils play a central role in mediating chronic, Th2-driven ileitis that is dependent on intestinal IL33 induced by the gut microbiome.[34] In the present study, we found that expansion of peripheral BM-derived eosinophils, defined as $CD11b^{+}$Siglec-F^{+} cells (Supplementary Figure 6), is already present in 4-week-old SAMP, before the appearance of gastritis, compared with age-matched AKR (Figure 5*A*). This trend is consistent with what was previously observed in older SAMP,[34] when intestinal-like metaplasia is fully established, and is increased vs 4-week-old SAMP. Locally, baseline presence of eosinophils identified by MBP, one of the most prevalent proteins specifically-produced by eosinophils,[45,46] is detected in young SAMP and also found in equal numbers in age-matched AKR (Figure 5*B*). As disease progresses, the number of infiltrating MBP^{+} eosinophils greatly increases, first appearing at the margination between the submucosa and muscularis mucosa and then collecting at the base of the gastric glands with infiltrates percolating upwards throughout the LP vs AKRs, wherein eosinophils are scarce and sparsely detected (Figure 5*B*). Quantitatively, MBP^{+} eosinophils are clearly evident in SAMP corpus as intestinalizing SPEM progresses, showing a 4-fold increase by 20 weeks compared with AKR (Figure 5*B*).

These results indicate that systemic expansion of eosinophils and their recruitment into gastric tissues occurs early and is sustained in SAMP with advanced intestinalized SPEM. Significant abrogation of BM-derived eosinophils (Figure 5*A*) and subsequent decreased recruitment into the gastric mucosa of SAMP lacking IL33 (SAMPx*Il33*$^{-/-}$)

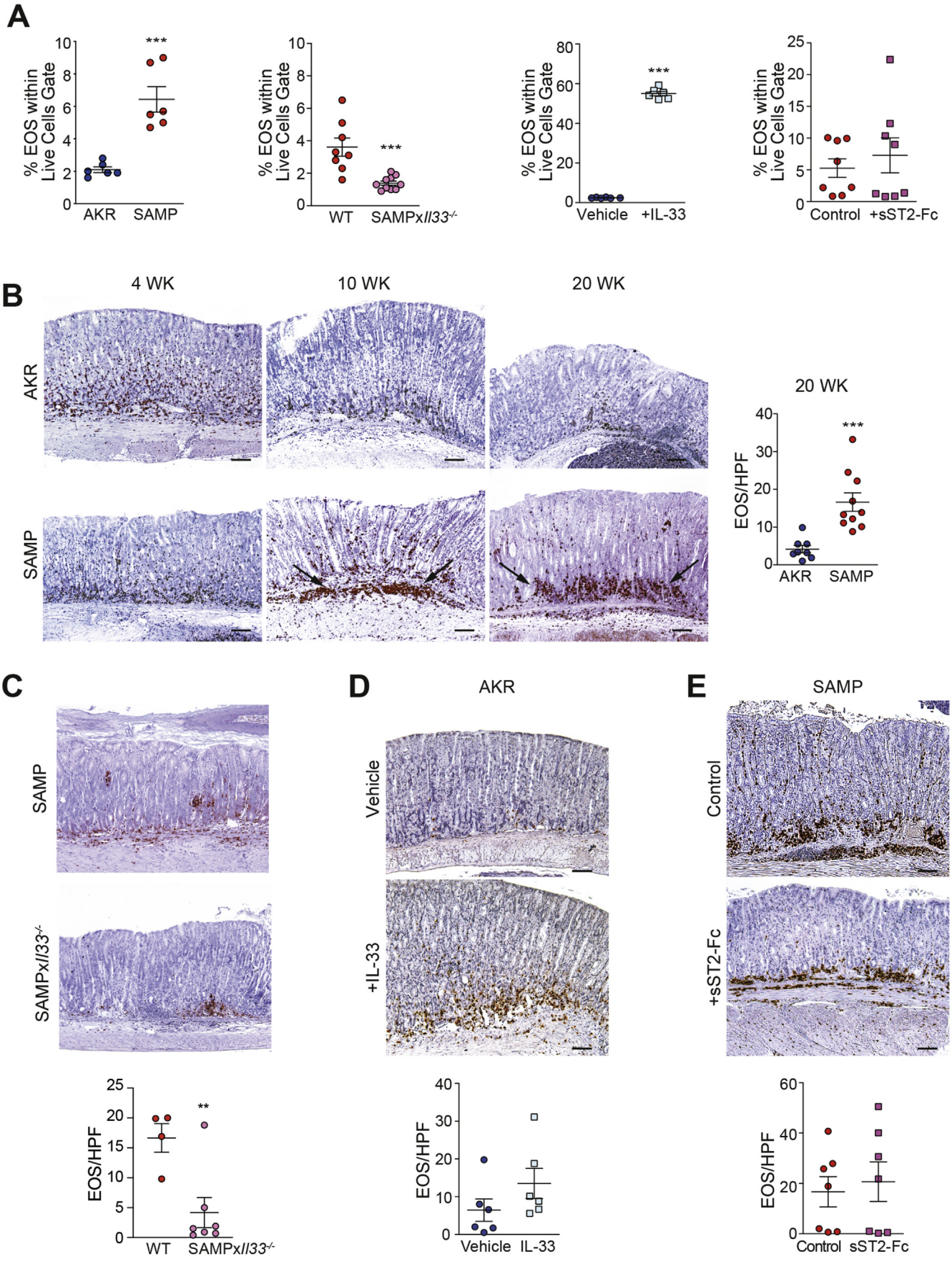
A
% EOS within Live Cells Gate
AKR
SAMP
WT
SAMPx/l33-/-
Vehicle
+IL-33
Control
+sST2-Fc
B
4 WK
10 WK
20 WK
AKR
SAMP
EOS/HPF
C
SAMP
SAMPx/l33-/-
D
AKR
Vehicle
+IL-33
E
SAMP
Control
+sST2-Fc
sST2-Fc

compared with wild-type littermates (SAMPx*Il33*$^{+/+}$) (Figure 5*C*) confirm the early reliance on IL33 for these effects.

Eosinophil expansion, in fact, can be dramatically elicited, particularly in the periphery, in healthy AKR after acute (1 week) IL33 administration. Likewise, aside from the striking mucosal epithelial alterations described above (Figure 2), IL33 also promotes a trend of eosinophil recruitment into the corpus of treated AKR (Figure 5*D*). These results indicate that in the absence of inflammation, exogenous IL33 induces robust systemic expansion, and to a lesser extent, local recruitment of eosinophils into the gastric mucosa. Interestingly, IL33 blockade in SAMP with established disease does not affect expansion of BM-derived eosinophils (Figure 5*A*) or local recruitment of MBP^{+} eosinophils (Figure 5*E*), indicating that once these processes are induced, particularly in mice exposed to chronic inflammatory conditions, they cannot be reversed.

Eosinophil Depletion Effectively Reduces Gastritis, Infiltration of M2 Macrophages, and Intestinalized Spasmolytic Polypeptide-Expressing Metaplasia

Because IL33 blockade is effective in dampening both infiltration of CD163^{+} M2 macrophages as well as intestinal-like metaplasia, but not recruitment of eosinophils in SAMP, we tested whether earlier intervention of eosinophil depletion has downstream effects on advanced intestinalized SPEM. As such, 14-week-old SAMP were treated with antibodies against CCR3 and IL5, alone and in combination, previously shown to effectively deplete eosinophils.[34,47,48] Eosinophil depletion was confirmed in both peripheral BM and corpus tissues (Supplementary Figures 7*A* and 6*A*, *left panels*), with histologic evaluation showing global improvement in restoring normal epithelial architecture, reducing the presence of cellular immune infiltrates, and decreasing overall inflammation within the LP and hyperplasia of muscle wall layers in mice treated with anti-IL5 and anti-CCR3, alone and in combination, vs IgG-treated controls (Figure 6*A* and *C*). Eosinophil depletion is also able to effectively decrease the presence of infiltrating IL33-expressing M2 macrophages (Figure 6*A* and *D* and Supplementary Figure 7*B*) and potently reduces gene expression of M2-associated molecules (Supplementary Figure 7*C*), but does not affect epithelial-derived IL33 (Supplementary Figure 7*D*).

Importantly, CD44v colabeling with GSII and GIF reveals that while no dramatic differences are observed in GSII among experimental groups, increased intensity of GIF is noted, particularly in SAMP treated with anti-IL5 or combination anti-IL5/anti-CCR3 vs controls, indicating at least partial reversal of oxyntic atrophy (Figure 6*A*, *right panels*). Interestingly, the decreased *Mist1* seen during SPEM is dramatically reversed after eosinophil depletion (Figure 6*E*), suggesting eosinophil-dependent chief cell transdifferentiation during SPEM. Taken together, these results indicate an essential role for eosinophils in the development of intestinalized SPEM.

Discussion

Increasing evidence confirms the importance of the IL33/ST2 axis in the development of gastritis and gastric cancer; in this context, IL33 is an ideal candidate to link these two processes. However, although several studies have reported associative findings in patients, correlating increased IL33 with intestinal-type gastric cancer[18] and poor prognostic factors,[15,49] less is known regarding specific IL33-dependent mechanisms leading to these pathologies. Based on the published literature and data from the present study, we propose a working hypothesis regarding the mechanistic role of IL33 in promoting SPEM progression and the gastritis-metaplasia-dysplasia-carcinoma sequelae in which eosinophils play a central role.

Some consider SPEM/intestinalized SPEM is a mandatory step for dysplasia, and eventually carcinoma, to proceed.[50] Once established, intestinalized SPEM or intestinal metaplasia, or both, may not be reversible in the presence of inciting factors such as chronic inflammation.[51] In fact, along with distinct gastric epithelial changes, an essential component to attain intestinal-like characteristics is nonresolving chronic inflammation, often thought to be dependent on *H pylori* status.[51,52] In this setting, IL33 represents a critical mediator for SPEM/intestinalized SPEM to manifest, considering its ability to both potently stimulate epithelial proliferation and metaplasia as well as induce and sustain chronic Th2-driven inflammation.

Our data show that the most prevalent form of IL33 in SAMP with established disease is bioactive fIL33, which is released during chronic inflammation, with minimal presence of the less bioactive cleaved form (cIL33)[38–40] that is more highly expressed in uninflamed AKR stomachs. In uninflamed young mice (AKR/SAMP) and older AKR, nuclear sequestration occurs within gastric epithelial cells, serving as reservoirs for IL33 that is readily available for immediate release upon exposure to appropriate stimuli.[18] In fact, under homeostatic conditions, the primary role of IL33 in the GI tract is believed to be epithelial repair and restitution and to promote overall mucosal wound healing.[33,53]

Interestingly, we found that at the transcript level, *Il33* is significantly decreased in SAMP compared with AKR, which likely reflects a negative feedback mechanism in response to high systemic IL33. In line with this finding, *Il33* is also

Figure 5. Early IL33-dependent peripheral expansion and increased eosinophil recruitment to SAMP stomachs. (*A*) Percentages of BM-derived eosinophils (EOS), and representative immunohistochemistry photomicrographs of corpus from (*B*) SAMP vs AKR, (*C*) SAMPx*Il33*$^{-/-}$ vs wild-type littermates, (*D*) IL-33- vs vehicle-treated AKR, and (*E*) sST2-Fc- vs IgG-treated SAMP, stained for MBP and eosinophil counts (N = 4-10). HPF, high-power field. Original magnification ×10+1.25; *scale bars*: 100 μm. $^{**}P < .01$, $^{***}P < .001$.

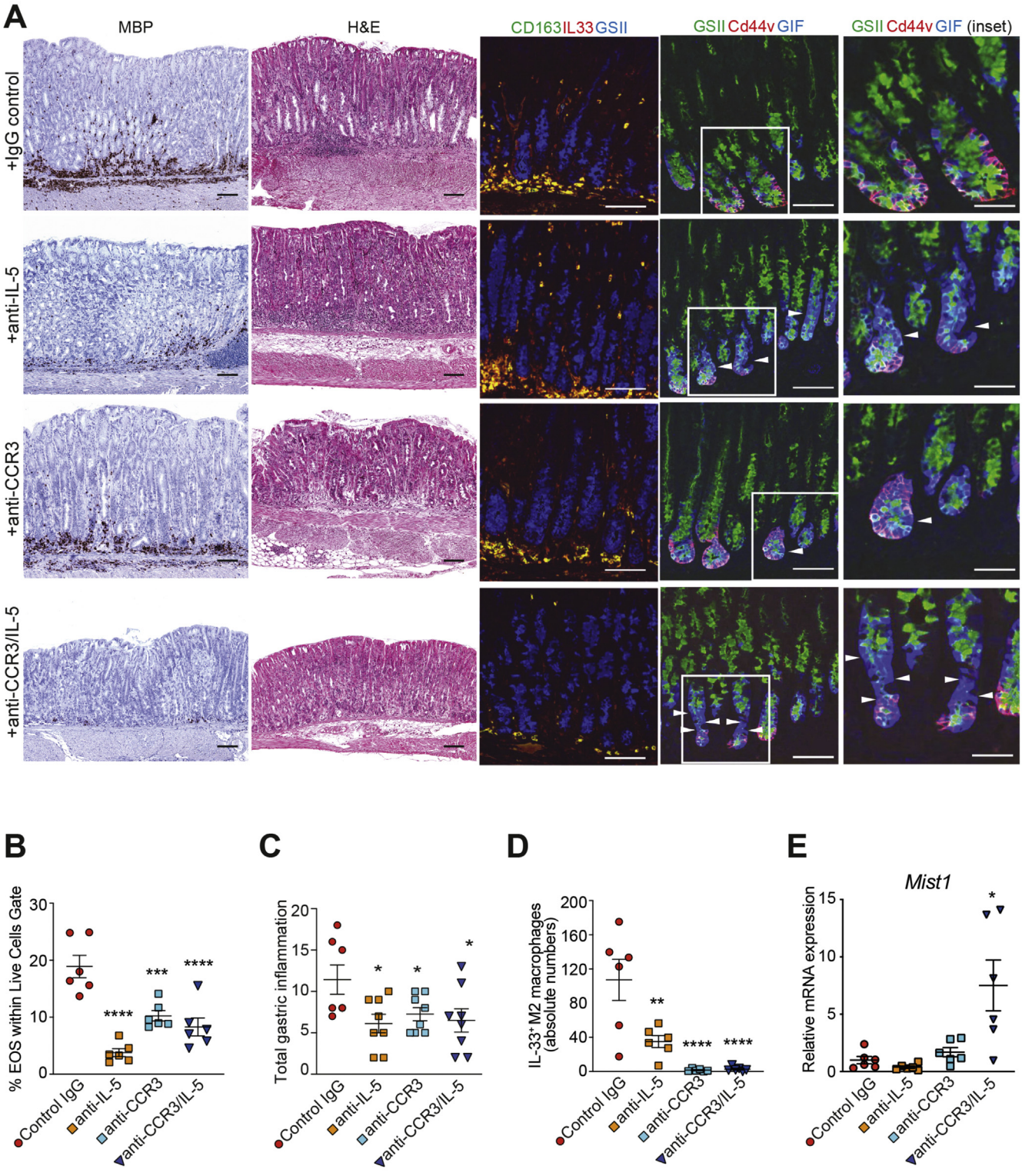

Figure 6. Eosinophil depletion reduces gastritis, M2 macrophage recruitment, and SPEM in SAMP. (*A*) Representative photomicrographs of corpus stained (left-to-right): for MBP (eosinophils), with H&E, and by immunofluorescence for IL33- (*red*) expressing CD163^{+} (*green*) M2 macrophages (*yellow*), showing reduction after anti-IL5, anti-CCR3 or combination anti-IL5/CCR3, and for GSII (*green*), CD44v (*red*) and GIF (*blue*) showing specific increase in GIF (*arrowheads*), suggesting protection from oxyntic atrophy. Original magnification ×20 and ×40 (*insets*); *scale bars*: 100 μm, 50 μm (*insets*). Quantitation of gastric (*B*) eosinophils, (*C*) inflammation, (*D*) IL33-expressing M2 macrophages, and (*E*) *Mist1* after eosinophil depletion. Data are representative of 3 experiments (N = 7-8 per experiment). *$P < .05$, **$P < .01$; ***$P < .001$; ****$P < .0001$.

decreased after exogenous IL33 administration, whereas the *Il1rl1* variant coding for sST2 (soluble decoy receptor) is greatly increased, which together serve to downregulate overall IL33 bioactivity.

The present study also introduces the SAMP mouse strain as a model of intestinalized SPEM that develops spontaneously and progresses in severity, without chemical, genetic, or immunologic manipulation. These mice provide an ideal tool to investigate the natural course of disease and a convenient system to test potential preclinical therapies for preneoplastic conditions that may lead to gastric cancer, in which preventive and therapeutic strategies can both be effectively implemented.

Using a therapeutic approach, we found that IL33 neutralization by sST2-Fc administration is effective at reversing intestinalized SPEM, primarily by targeting the epithelial compartment and reducing IL33-dependent epithelial alterations, which are hallmark features of metaplasia. In addition, IL33 blockade decreases the severity of chronic gastritis and the presence of M2 macrophages, which are also characteristic of metaplasia and progression to intestinalized SPEM.[31]

Importantly, using SAMP, we not only demonstrate the essential role for IL33 in the development of intestinal-like metaplasia but also that the IL33/ST2 axis is important for several steps throughout this process. For example, IL33 clearly has direct effects on epithelial cells. Indeed, epithelial alterations within the GI tract were among the initial aberrancies described after healthy mice were exposed to high levels of IL33.[9] We and others[41] confirmed these observations in the stomach, showing that rIL33 induces severe oxyntic atrophy and upregulates specific markers of SPEM. Alternatively, IL33 also has profound effects on the gastric immune compartment, promoting, for example, vigorous infiltration of eosinophils and M2 macrophages,[31] further perpetuating a chronic inflammatory state. Importantly, prolonged and elevated levels of IL33 have the ability to sustain chronic inflammation in the stomach, which is essential for intestinal metaplasia to advance to gastric cancer.

The results of our study also underscore the importance of eosinophils in the development of intestinal-like metaplasia and that IL33 plays a critical role in the systemic expansion and early recruitment of eosinophils into the gastric mucosa of SAMP as well as AKRs treated with rIL33. Previously, eosinophils in gastric metaplasia and cancer development have been proposed to have both pathogenic as well as protective functions. A prior study investigating early gastric cancers demonstrated the presence of tumor stromal eosinophils with morphologic evidence of activation as well as tumor cells in intimate contact with activated eosinophils with focal cytopathic changes.[54]

Gastric carcinomas have also been reported to express eosinophil-associated chemotactic cytokines, including IL2, IL5, and granulocyte-macrophage colony–stimulating factor, with expression of granulocyte-macrophage colony–stimulating factor appearing to be specific for signet ring carcinoma cells.[55] On the other hand, in support of a protective function, high preoperative eosinophil counts were found to correlate with prolonged survival after surgery,[56] and the-28G polymorphism in the promoter region of the eosinophil chemoattractant RANTES (regulated upon activation normal T cell expressed and secreted) is associated with a reduced risk of developing severe intestinal metaplasia.[57]

Nonetheless, while our results indicate that eosinophils play an important role during early events leading to gastritis/metaplasia, one can certainly speculate that other IL33-responsive innate immune cell populations may also contribute. Our data show that IL33 can promote local recruitment of M2 macrophages that themselves are potent producers of IL33. These findings are in line with previous reports demonstrating the ability of IL33 to increase overall macrophage numbers in the stomach and to polarize them to an alternatively activated M2 phenotype, albeit in the periphery (peritoneum),[41] and that M2 macrophages are dramatically reduced in IL33-deficient mice in which advanced SPEM has been elicited, but that can also be rescued by administering rIL13.[31]

Our findings in SAMP, however, indicate that M2 macrophage infiltration is likely downstream of eosinophil activation and recruitment because eosinophil depletion, similar to systemic IL33 blockade, has a significant impact on reducing the infiltration of gastric M2 macrophages that also happen to produce IL33. Interestingly, however, eosinophil depletion does not appear to have an effect on IL33 expression in the gastric epithelium of SAMP. In contrast, L635-induced SPEM does not appear to require eosinophils,[31] which may simply reflect differences in inciting factors between the 2 models (ie, chemical obliteration of parietal cells vs chronic, nonresolving inflammation).

An alternative hypothesis is that ILC2s are also an IL33-responsive innate immune cell population that can affect SPEM. ILC2s have not been detected or isolated from gastric tissues until recently, when Li et al[58] reported the prevalence of GATA-3^{+}Lin^{-} cells in tumors of patients with *H pylori*-associated gastric cancer. Of note, and counterintuitive to this finding, Buzzelli et al[41] showed that IL33 is rapidly induced after acute *H pylori* infection but suppressed in chronic infection. However, in the former study, it is unclear what the IL33 levels were, whether they correlated with GATA-3^{+}Lin^{-} ILC2 frequency, and whether IL33 exhibited temporal changes during early vs late stages in different types of gastric cancers. In the latter study, acute vs chronic *H pylori* infection was defined as 1 and 7 days vs 2 months, which may not reflect chronic infection, especially in gastric cancer-susceptible individuals.

Although indirect evidence suggests emergence of gastric ILC2s in IL33-treated mice,[41] we recently reported increased ILC2s after L635-dependent acute gastric injury.[59] Similarly, preliminary data in SAMP mice also show an increased frequency, albeit quite low, of ILC2s vs AKR (Supplementary Figure 8); however, whether ILC2s contribute to the SAMP gastric phenotype is unknown. On the basis of studies characterizing SAMP lacking T/B cells, but with intact ILC function (ie, SAMPx*Rag2*$^{-/-}$ strain), ILCs likely play a negligible role in SPEM development because these mice, without the ability to mount adaptive immune

responses and sustain a chronic inflammatory state, have virtually normal stomachs (Supplementary Figure 8).

Finally, yet another IL33-responsive innate immune cell population (ie, mast cells) has been recently implicated in the development of gastric cancer in *gp130*$^{F/F}$ mice, specifically through mobilization of macrophages.[18] Although similar to early IL33-dependent activation of eosinophils upstream of macrophage recruitment, the precise temporal involvement of mast cells and their interaction(s) with other mucosal populations to promote events leading to intestinal metaplasia and gastric cancer is unclear.

Taken together, the present study underscores a critical role for IL33 in the development of chronic inflammation and metaplasia in the stomach and implicates eosinophils as an early IL33-responsive innate immune cell population that participates in the complex orchestration leading to SPEM/intestinalized SPEM. As such, targeting the IL33/ST2 axis for future therapeutic modalities to interrupt the early initial events leading to gastritis and metaplasia and potentially reversing intestinalizing SPEM may prove to be beneficial for the prevention or treatment, or both, of patients susceptible to gastric cancer.

Supplementary Material

Note: To access the supplementary material accompanying this article, visit the online version of *Gastroenterology* at www.gastrojournal.org, and at https://doi.org/10.1053/j.gastro.2020.09.040.

References

1. Balkwill F, Mantovani A. Inflammation and cancer: back to Virchow? Lancet 2001;357:539–545.
2. Crusz SM, Balkwill FR. Inflammation and cancer: advances and new agents. Nat Rev Clin Oncol 2015; 12:584–596.
3. Mantovani A, Barajon I, Garlanda C. IL-1 and IL-1 regulatory pathways in cancer progression and therapy. Immunol Rev 2018;281:57–61.
4. Lopetuso LR, Chowdhry S, Pizarro TT. Opposing functions of classic and novel IL-1 family members in gut health and disease. Front Immunol 2013;4:181.
5. Maywald RL, Doerner SK, Pastorelli L, et al. IL-33 activates tumor stroma to promote intestinal polyposis. Proc Natl Acad Sci U S A 2015;112:E2487–E2496.
6. Malik A, Sharma D, Zhu Q, et al. IL-33 regulates the IgA-microbiota axis to restrain IL-1alpha-dependent colitis and tumorigenesis. J Clin Invest 2016;126:4469–4481.
7. **He Z, Chen L,** Souto FO, et al. Epithelial-derived IL-33 promotes intestinal tumorigenesis in Apc(Min/+) mice. Sci Rep 2017;7:5520.
8. Venerito M, Nardone G, Selgrad M, et al. Gastric cancer-epidemiologic and clinical aspects. Helicobacter 2014; 19(Suppl 1):32–37.
9. Schmitz J, Owyang A, Oldham E, et al. IL-33, an interleukin-1-like cytokine that signals via the IL-1 receptor-related protein ST2 and induces T helper type 2-associated cytokines. Immunity 2005;23:479–490.
10. Pastorelli L, Garg RR, Hoang SB, et al. Epithelial-derived IL-33 and its receptor ST2 are dysregulated in ulcerative colitis and in experimental Th1/Th2 driven enteritis. Proc Natl Acad Sci U S A 2010;107:8017–8022.
11. **Neill DR, Wong SH,** Bellosi A, et al. Nuocytes represent a new innate effector leukocyte that mediates type-2 immunity. Nature 2010;464:1367–1370.
12. Joshi AD, Oak SR, Hartigan AJ, et al. Interleukin-33 contributes to both M1 and M2 chemokine marker expression in human macrophages. BMC Immunology 2010;11:52.
13. Stolarski B, Kurowska-Stolarska M, Kewin P, et al. IL-33 exacerbates eosinophil-mediated airway inflammation. J Immunol 2010;185:3472–3480.
14. **Hung LY, Lewkowich IP,** Dawson LA, et al. IL-33 drives biphasic IL-13 production for noncanonical Type 2 immunity against hookworms. Proc Natl Acad Sci U S A 2013;110:282–287.
15. **Sun P, Ben Q,** Tu S, et al. Serum interleukin-33 levels in patients with gastric cancer. Dig Dis Sci 2011;56:3596–3601.
16. Ye XL, Zhao YR, Weng GB, et al. IL-33-induced JNK pathway activation confers gastric cancer chemotherapy resistance. Oncol Rep 2015;33:2746–2752.
17. Yu XX, Hu Z, Shen X, et al. IL-33 promotes gastric cancer cell invasion and migration via ST2-ERK1/2 pathway. Dig Dis Sci 2015;60:1265–1272.
18. Eissmann MF, Dijkstra C, Jarnicki A, et al. IL-33-mediated mast cell activation promotes gastric cancer through macrophage mobilization. Nat Commun 2019; 10:2735.
19. Correa P. A human model of gastric carcinogenesis. Cancer Res 1988;48:3554–3560.
20. Saenz JB, Mills JC. Acid and the basis for cellular plasticity and reprogramming in gastric repair and cancer. Nat Rev Gastroenterol Hepatol 2018;15:257–273.
21. Goldenring JR. Pyloric metaplasia, pseudopyloric metaplasia, ulcer-associated cell lineage and spasmolytic polypeptide-expressing metaplasia: reparative lineages in the gastrointestinal mucosa. J Pathol 2018;245:132–137.
22. Schmidt PH, Lee JR, Joshi V, et al. Identification of a metaplastic cell lineage associated with human gastric adenocarcinoma. Lab Invest 1999;79:639–646.
23. **Nam KT, Lee HJ,** Sousa JF, et al. Mature chief cells are cryptic progenitors for metaplasia in the stomach. Gastroenterology 2010;139:2028–2037.
24. Mills JC, Sansom OJ. Reserve stem cells: Differentiated cells reprogram to fuel repair, metaplasia, and neoplasia in the adult gastrointestinal tract. Sci Signal 2015;8:re8.
25. Radyk MD, Burclaff J, Willet SG, et al. Metaplastic cells in the stomach arise, independently of stem cells, via dedifferentiation or transdifferentiation of chief cells. Gastroenterology 2018;154:839–843.
26. Lennerz JK, Kim SH, Oates EL, et al. The transcription factor MIST1 is a novel human gastric chief cell marker whose expression is lost in metaplasia, dysplasia, and carcinoma. Am J Pathol 2010; 177:1514–1533.

27. Burclaff J, Osaki LH, Liu D, et al. Targeted apoptosis of parietal cells is insufficient to induce metaplasia in stomach. Gastroenterology 2017;152:762–766.
28. **Willet SG, Lewis MA,** Miao ZF, et al. Regenerative proliferation of differentiated cells by mTORC1-dependent paligenosis. EMBO J 2018;37:e98311.
29. Weis VG, Sousa JF, LaFleur BJ, et al. Heterogeneity in mouse spasmolytic polypeptide-expressing metaplasia lineages identifies markers of metaplastic progression. Gut 2013;62:1270–1279.
30. Petersen CP, Weis VG, Nam KT, et al. Macrophages promote progression of spasmolytic polypeptide-expressing metaplasia after acute loss of parietal cells. Gastroenterology 2014;146:1727–1738.
31. Petersen CP, Meyer AR, De Salvo C, et al. A signalling cascade of IL-33 to IL-13 regulates metaplasia in the mouse stomach. Gut 2018;67:805–817.
32. Reuter BK, Pastorelli L, Brogi M, et al. Spontaneous, immune-mediated gastric inflammation in SAMP1/YitFc mice, a model of Crohn's-like gastritis. Gastroenterology 2011;141:1709–1719.
33. Lopetuso LR, De Salvo C, Pastorelli L, et al. IL-33 promotes recovery from acute colitis by inducing miR-320 to stimulate epithelial restitution and repair. Proc Natl Acad Sci U S A 2018;115:E9362–E9370.
34. De Salvo C, Wang XM, Pastorelli L, et al. IL-33 drives eosinophil infiltration and pathogenic type 2 helper T-cell immune responses leading to chronic experimental ileitis. Am J Pathol 2016;186:885–898.
35. Arseneau KKO, Cominelli F. Improving the reproducibility and quality of reporting for animal studies in inflammatory bowel disease. Inflamm Bowel Dis 2017;23:2069–2071.
36. Turani H, Lurie B, Chaimoff C, et al. The diagnostic significance of sulfated acid mucin content in gastric intestinal metaplasia with early gastric cancer. Am J Gastroenterol 1986;81:343–345.
37. Nozaki K, Ogawa M, Williams JA, et al. A molecular signature of gastric metaplasia arising in response to acute parietal cell loss. Gastroenterology 2008;134:511–522.
38. Talabot-Ayer D, Lamacchia C, Gabay C, et al. Interleukin-33 is biologically active independently of caspase-1 cleavage. J Biol Chem 2009;284:19420–19426.
39. Cayrol C, Girard JP. The IL-1-like cytokine IL-33 is inactivated after maturation by caspase-1. Proc Natl Acad Sci U S A 2009;106:9021–9026.
40. **Luthi AU, Cullen SP,** McNeela EA, et al. Suppression of interleukin-33 bioactivity through proteolysis by apoptotic caspases. Immunity 2009;31:84–98.
41. Buzzelli JN, Chalinor HV, Pavlic DI, et al. IL33 Is a stomach alarmin that initiates a skewed Th2 response to injury and infection. Cell Mol Gastroenterol Hepatol 2015;1:203–221.
42. **Wada T, Ishimoto T,** Seishima R, et al. Functional role of CD44v-xCT system in the development of spasmolytic polypeptide-expressing metaplasia. Cancer Sci 2013;104:1323–1339.
43. Fagundes CT, Amaral FA, Souza AL, et al. ST2, an IL-1R family member, attenuates inflammation and lethality after intestinal ischemia and reperfusion. J Leukoc Biol 2007;81:492–499.
44. Miao ZF, Adkins-Threats M, Burclaff JR, et al. A metformin-responsive metabolic pathway controls distinct steps in gastric progenitor fate decisions and maturation. Cell Stem Cell 2020;26:910–925.
45. Mishra A, Hogan SP, Lee JJ, et al. Fundamental signals that regulate eosinophil homing to the gastrointestinal tract. J Clin Invest 1999;103:1719–1727.
46. Hogan SP, Rosenberg HF, Moqbel R, et al. Eosinophils: biological properties and role in health and disease. Clin Exp Allergy 2008;38:709–750.
47. Masterson JC, McNamee EN, Jedlicka P, et al. CCR3 blockade attenuates eosinophilic ileitis and associated remodeling. Am J Pathol 2011;179:2302–2314.
48. Song DJ, Shim MH, Lee N, et al. CCR3 monoclonal antibody inhibits eosinophilic inflammation and mucosal injury in a mouse model of eosinophilic gastroenteritis. Allergy Asthma Immunol Res 2017;9:360–367.
49. Hu W, Li X, Li Q, et al. Interleukin-33 expression does not correlate with survival of gastric cancer patients. Pathol Oncol Res 2017;23:615–619.
50. Fox JG, Wang TC. Inflammation, atrophy, and gastric cancer. J Clin Invest 2007;117:60–69.
51. Correa P, Piazuelo MB. The gastric precancerous cascade. J Dig Dis 2012;13:2–9.
52. Petersen CP, Mills JC, Goldenring JR. Murine models of gastric corpus preneoplasia. Cell Mol Gastroenterol Hepatol 2017;3:11–26.
53. Monticelli LA, Osborne LC, Noti M, et al. IL-33 promotes an innate immune pathway of intestinal tissue protection dependent on amphiregulin-EGFR interactions. Proc Natl Acad Sci U S A 2015;112:10762–10767.
54. Caruso RA, Giuffre G, Inferrera C. Minute and small early gastric carcinoma with special reference to eosinophil infiltration. Histol Histopathol 1993;8:155–166.
55. Hong SW, Cho MY, Park C. Expression of eosinophil chemotactic factors in stomach cancer. Yonsei Med J 1999;40:131–136.
56. Iwasaki K, Torisu M, Fujimura T. Malignant tumor and eosinophils. I. Prognostic significance in gastric cancer. Cancer 1986;58:1321–1327.
57. Tahara T, Arisawa T, Shibata T, et al. Effect of RANTES promoter genotype on the severity of intestinal metaplasia in *Helicobacter* pylori-infected Japanese subjects. Dig Dis Sci 2009;54:1247–1252.
58. Li R, Jiang XX, Zhang LF, et al. Group 2 innate lymphoid cells are involved in skewed type 2 immunity of gastric diseases induced by *Helicobacter pylori* infection. Mediators Inflamm 2017;2017:4927964.
59. Meyer AR, Engevik AC Madorsky T, et al. Group 2 innate lymphoid cells coordinate damage response in the stomach. Gastroenterology. Published online September 3, 2020; doi:10.1053/j.gastro.2020.08.051.

Author names in bold designate shared co-first authorship.

Received November 6, 2019. Accepted September 22, 2020.

Correspondence
Address correspondence to: Theresa T. Pizarro, PhD, Department of Pathology, Case Western Reserve University School of Medicine, 2103 Cornell Road, WRB 5534, Cleveland, Ohio 44106. e-mail: theresa.pizarro@case.edu; fax: 216-368-0494.

Acknowledgments
We thank the following individuals for their important contributions to the manuscript: Xiao-Ming Wang, Danian Che, and Brian Marks for their technical support, as well as James J. Lee and Dirk E. Smith for provision of important reagents.

CRediT Authorship Contributions
Carlo De Salvo, PhD (Data curation: Lead; Formal analysis: Equal; Funding acquisition: Supporting; Investigation: Equal; Methodology: Lead; Writing – original draft: Lead). Luca Pastorelli, MD, PhD (Data curation: Equal; Formal analysis: Equal; Funding acquisition: Supporting; Investigation: Equal; Methodology: Equal; Visualization: Equal; Writing – original draft: Equal). Christine P. Petersen, PhD (Data curation: Supporting; Formal analysis: Supporting; Investigation: Supporting; Methodology: Supporting). Ludovica F. Buttò, PhD (Data curation: Supporting; Formal analysis: Supporting). Kristine A. Buela, PhD (Data curation: Supporting; Formal analysis: Supporting; Funding acquisition: Supporting; Investigation: Supporting; Methodology: Supporting). Sara Omenetti, PhD (Data curation: Supporting; Formal analysis: Supporting; Investigation: Supporting; Methodology: Supporting). Silviu A. Locovei, MD, PhD (Data curation: Supporting; Formal analysis: Supporting; Funding acquisition: Supporting). Shuvra Ray, MD, PhD (Data curation: Supporting; Methodology: Supporting). Hannah R. Friedman, undergraduate student (Data curation: Supporting; Funding acquisition: Supporting). Jacob Duijser, undergraduate student (Data curation: Supporting; Funding acquisition: Supporting). Hannah L. Wargo BS (Data curation: Supporting) Wei Xin, MD, PhD (Formal analysis: Supporting; Investigation: Supporting; Methodology: Supporting). Abdullah Osme, MD (Data curation: Supporting; Formal analysis: Supporting; Methodology: Lead). Fabio Cominelli, MD, PhD (Data curation: Supporting; Resources: Supporting; Supervision: Supporting). Ganapati H. Mahabeleshwar, PhD (Data curation: Supporting; Formal analysis: Supporting; Investigation: Supporting; Resources: Supporting). Jason Mills, MD, PhD (Data curation: Supporting; Funding acquisition: Supporting; Methodology: Supporting; Resources: Supporting; Supervision: Supporting; Writing – review & editing: Supporting). James Goldenring, MD, PhD (Data curation: Supporting; Formal analysis: Supporting; Funding acquisition: Supporting; Investigation: Supporting; Methodology: Supporting; Project administration: Supporting; Resources: Supporting; Supervision: Supporting; Writing – review & editing: Supporting). Theresa T. Pizarro, PhD (Conceptualization: Lead; Formal analysis: Lead; Funding acquisition: Lead; Investigation: Lead; Project administration: Lead; Resources: Lead; Supervision: Lead; Visualization: Lead; Writing – review & editing: Lead).

Conflicts of interest
The authors disclose no conflicts.

Funding
This work was supported by grants from the National Institutes of Health: DK056762, DK091222, DK042191, CA150964 Pilot & Feasibility Award (T.T.P.), DK071590 (J.R.G.), DK105129 (J.C.M.), a National Research Service Award F31 Predoctoral Fellowship DK104600 (C.P.P.), an Institutional T32 Fellowship from DK083251 (S.L.), as well as Cores from the Cleveland Silvio O. Conte Digestive Diseases Research Core Center (DK097948). Other funding sources include the DeGregorio Family Foundation (T.T.P.), the Department of Veterans Affairs: I01BX000930 (J.R.G.), the Crohn's & Colitis Foundation: RFA326877, CDA581292 (C.D.S.), RFA410354 (K.A.B), and SRFA592800 (H.R.F.), the American Gastroenterological Association: Eli & Edythe Broad Student Research Fellowship Award (H.R.F., J.D.), and the Italian Society of Gastroenterology (L.P.).

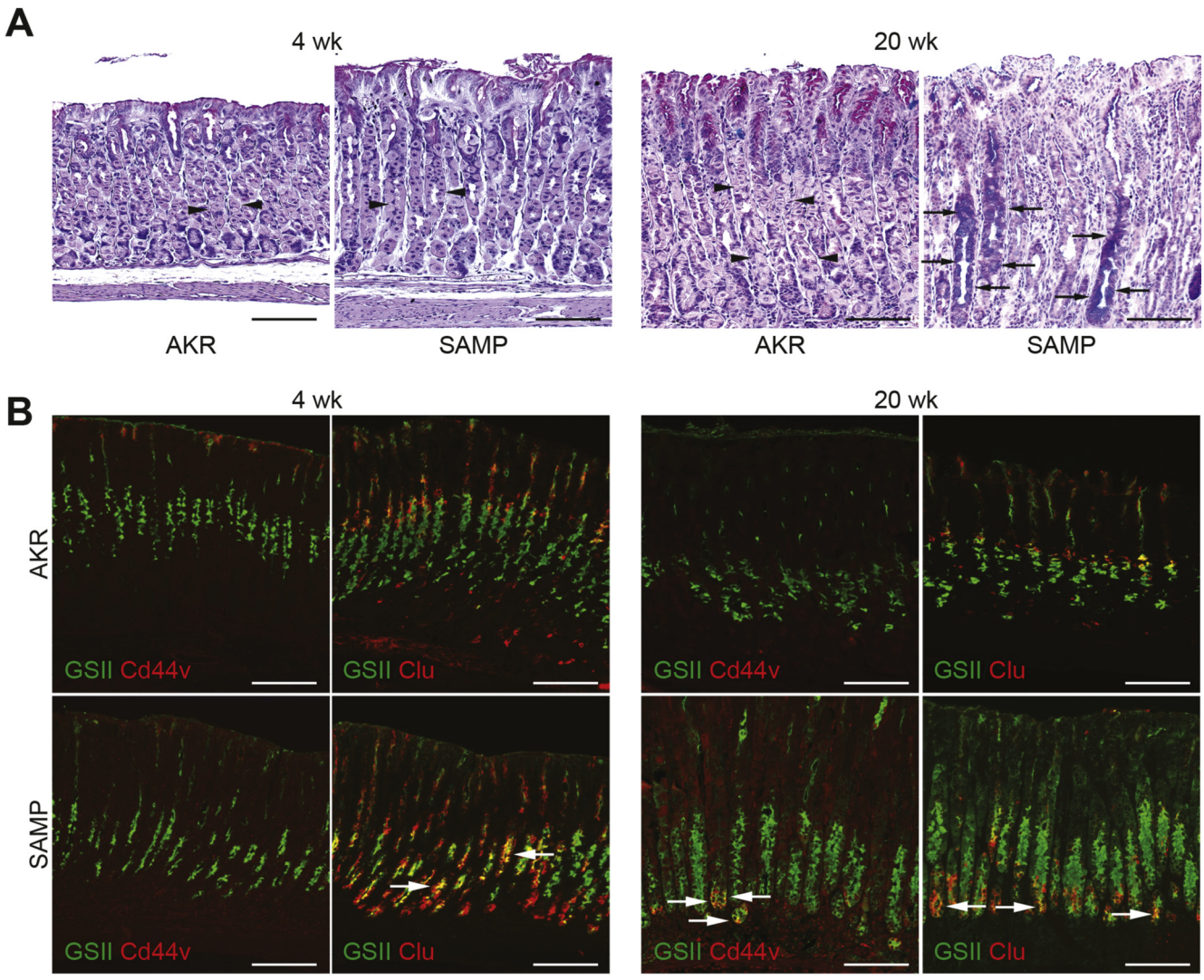

Supplementary Figure 1. Evidence of advanced intestinalized SPEM in stomachs of gastritis-prone SAMP mice. (*A*) Representative histologic image of 4-week-old SAMP shows early hyperproliferation of gastric glands compared with age-matched AKR (*left panels*), while in 20-week-old SAMP, Alcian blue/PAS staining highlights acidic mucin-secreting cells (*arrows*) replacing parietal (*arrowheads*) and chief cells as SPEM progresses, which is absent in age-matched AKR (*right panels*). Original magnification ×20+1.25; *scale bars*: 100 μm. (*B*) Representative immunofluorescent images of full-thickness corpus from 4-week-old SAMP display early, aberrant staining of GSII (*green*) and Clu (*red*), characteristic of SPEM (*left lower panels*) compared with age-matched AKR (*left upper panels*) that becomes more evident in 20-week-old SAMP with established gastritis, with clear abundance of $GSII^{+}$ cells and increased CD44v and Clu (both *red*), localizing to base of gastric glands (*arrows*, *right lower panels*) compared with age-matched AKR controls (*right upper panels*). Original magnification ×20; *scale bars*: 100 μm.

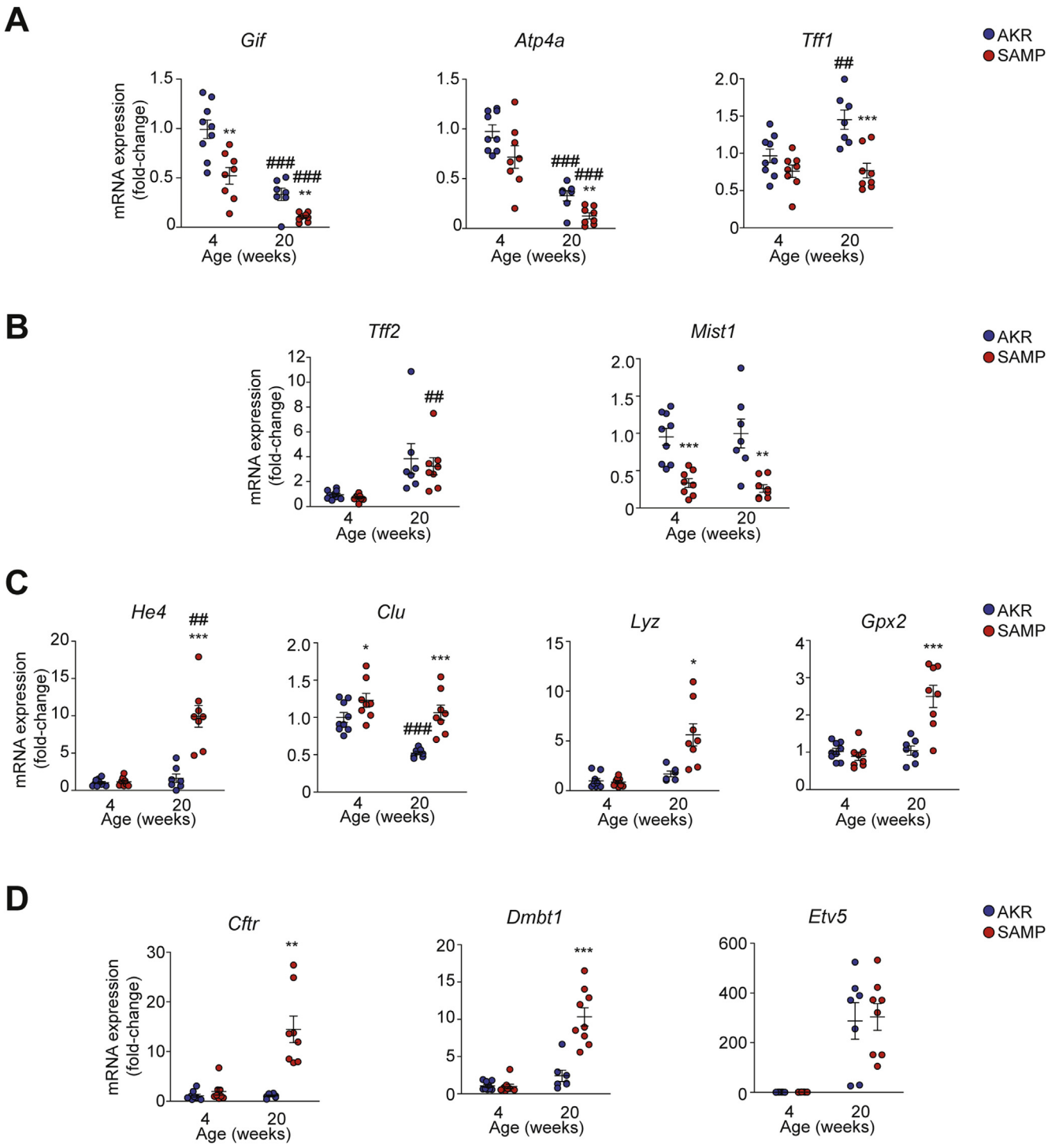

Supplementary Figure 2. Molecular profiling indicates advanced SPEM in SAMP corpus that progresses with age. Relative expression of (*A*) *Gif*, *Atp4a*, and *Tff1*, (*B*) *Tff2* and *Mist1*, (*C*) *He4*, *Clu*, *Lyz*, and *Gpx2*, and (*D*) *Cftr*, *Dmbt1*, and *Etv5* in young SAMP vs SAMP with established disease and vs age-matched AKR controls. Data are expressed as fold-change vs 4-week-old AKR (with mean arbitrarily set as 1) (N = 6-9). mRNA,2messenger RNA. **P* < .05, ***P* < .01, ****P*< .001 vs age-matched AKR; ##*P* < .01, ###*P* < .001 vs 4-week-old AKR/SAMP.

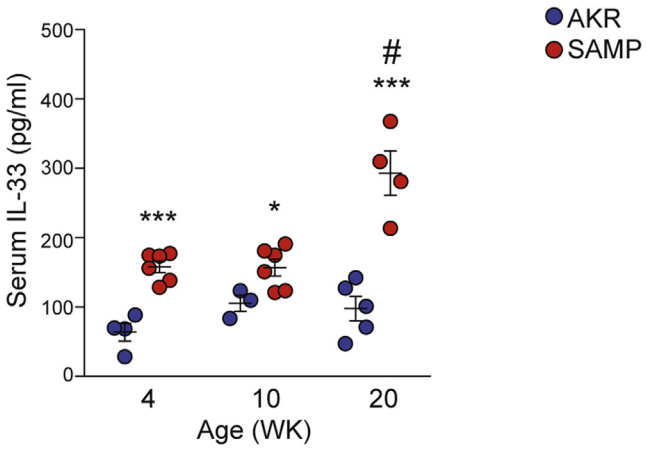

Supplementary Figure 3. Increased circulating levels of IL33 in SAMP mice. Serum levels of total IL33 protein in 4-, 10- and 20-week-old SAMP vs age-matched control AKR (N = 3-6). *$P < .05$, ***$P < .001$ vs age-matched AKR; #$P<0.05$ vs 4-week-old SAMP.

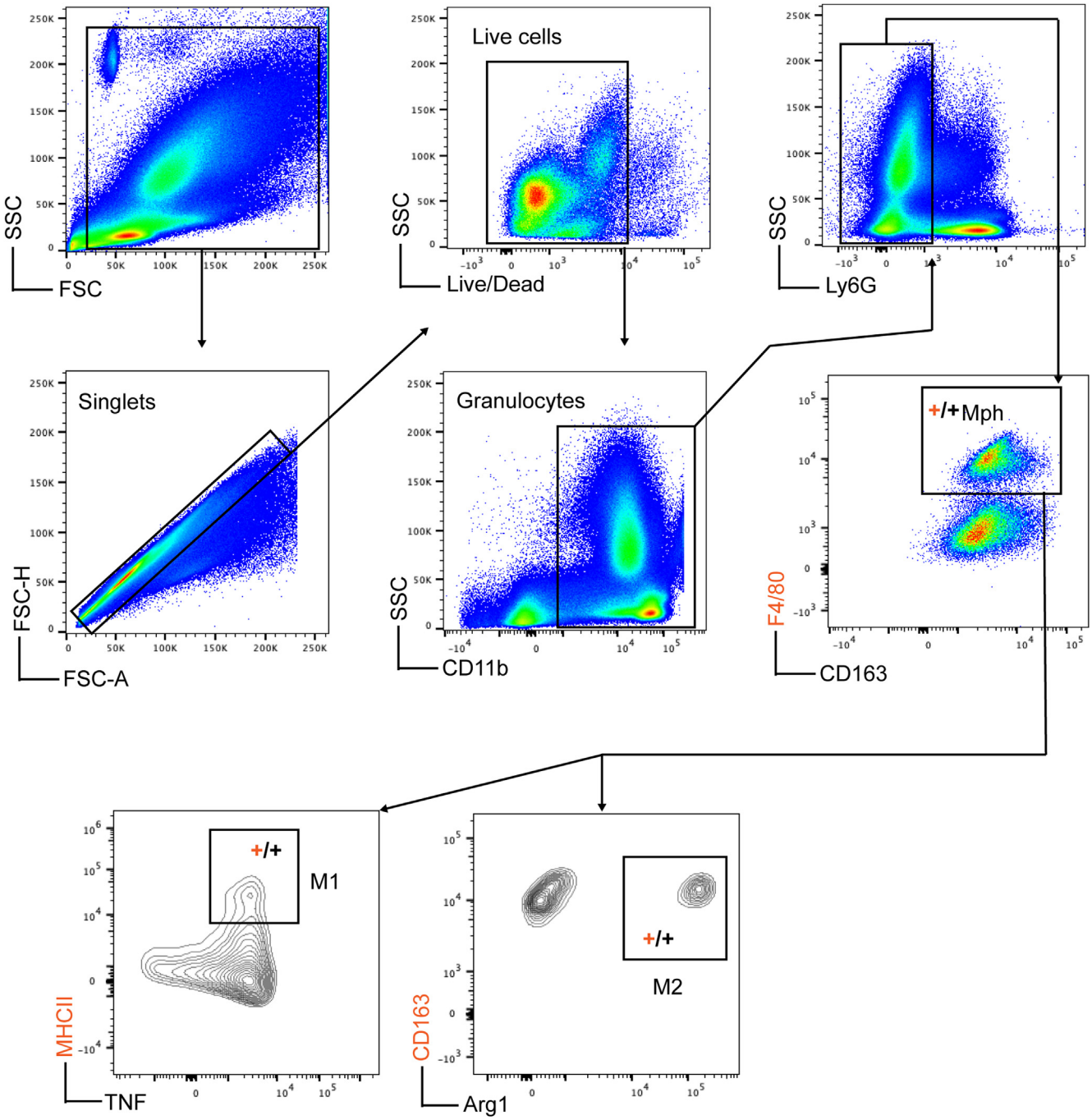

Supplementary Figure 4. Gating strategy for distinguishing M1 vs M2 macrophages by flow cytometry. Representative 2-dimensional dot plots (shown here for BM) for SAMP depict, from left-to-right: (1) side scatter (SSC) vs forward scatter (FSC) (gating on general cells), (2) FSC area (FAC-A) vs FSC height (FSC-H) (gating on singlets), (3) SSC area (SSC-A) vs live/dead (gating on live cells), (4) CD11b vs SSC-A (gating on granulocytes), (5) Ly6G vs SSC-A (gating on Ly6G^{-} cells), (6) CD163 vs F4/80 (gating on macrophages, Mph), and (7) tumor necrosis factor (TNF) vs major histocompatibility complex (MHC) II (gating on M1 macrophages), and Arg1 vs CD163 (gating on M2 macrophages).

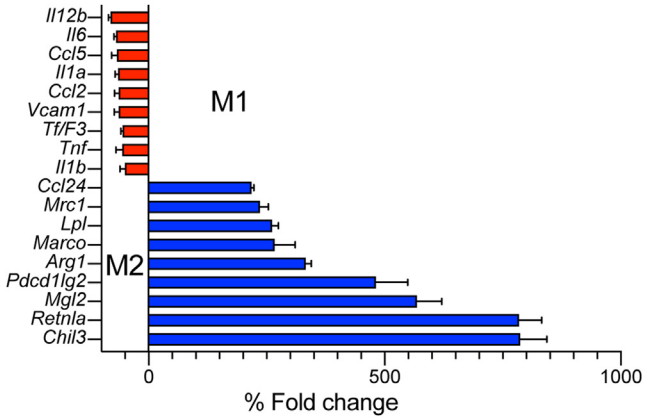

Supplementary Figure 5. Strong prominence of M2- vs M1-associated gene markers expressed in macrophages from SAMP vs AKR mice. Relative transcript levels of M1- vs M2-associated molecules (defined in Sica and Mantovani, Trends Immunol 2002 DOI: 10.1016/s1471-4906(02)02302-5; and Murray, Immunity 2017 DOI: 10.1146/annurev-physiol-022516-034339) in isolated macrophages from 10-week-old SAMP, normalized by *36B4* and expressed as percentage fold-change of age-matched AKR controls. Data are presented as mean ± SD (N = 6).

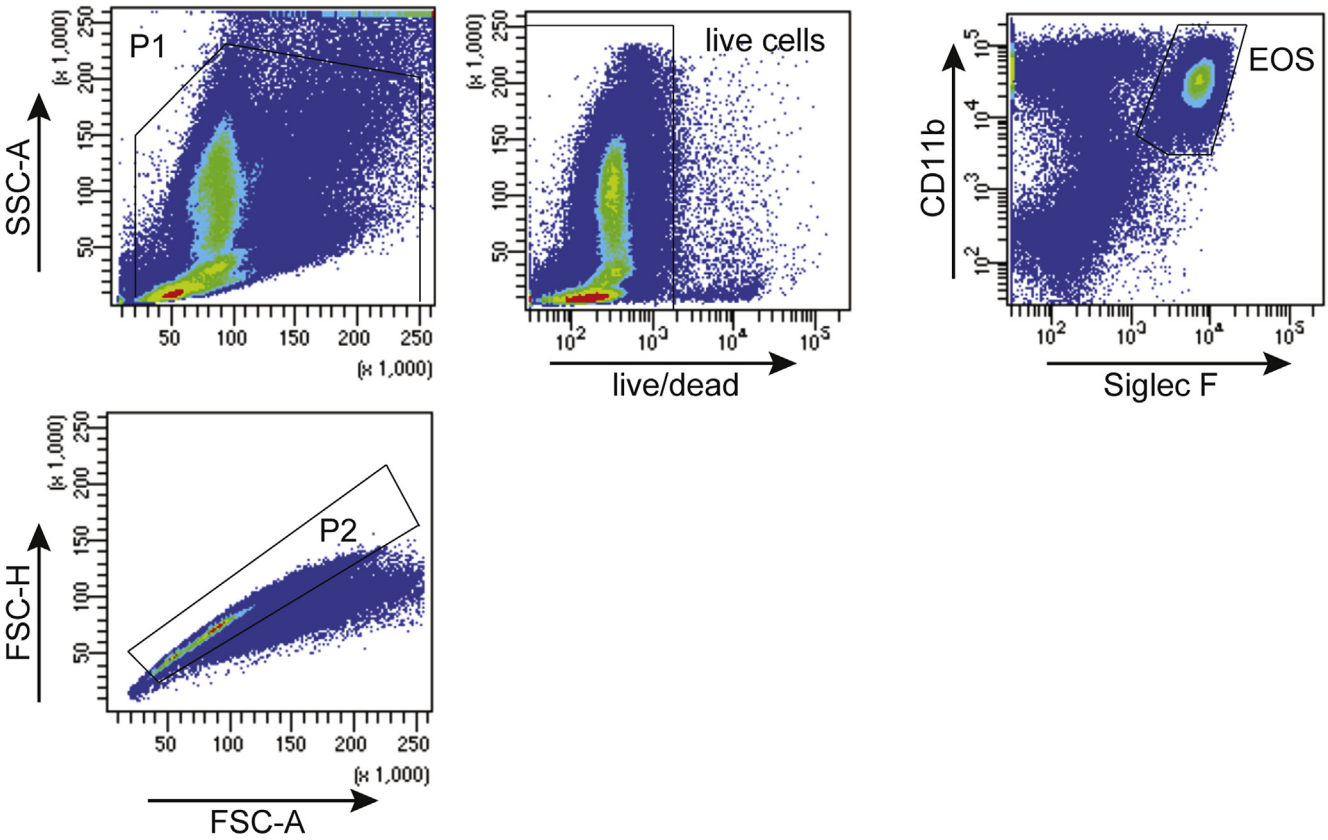

Supplementary Figure 6. Gating strategy for detecting eosinophils (EOS) by flow cytometry. Representative 2-dimensional dot plots (shown here for BM) for control AKR depict, from left-to-right: (1) side scatter (SSC) vs forward scatter (FSC) (P1, gating on general cells), (2) FSC area (FSC-A) vs FSC height (FSC-H) (P2, gating on singlets), (3) SSC area (SSC-A) vs live/dead (gating on live cells), and (4) CD11b vs Siglec-F (gating on eosinophils).

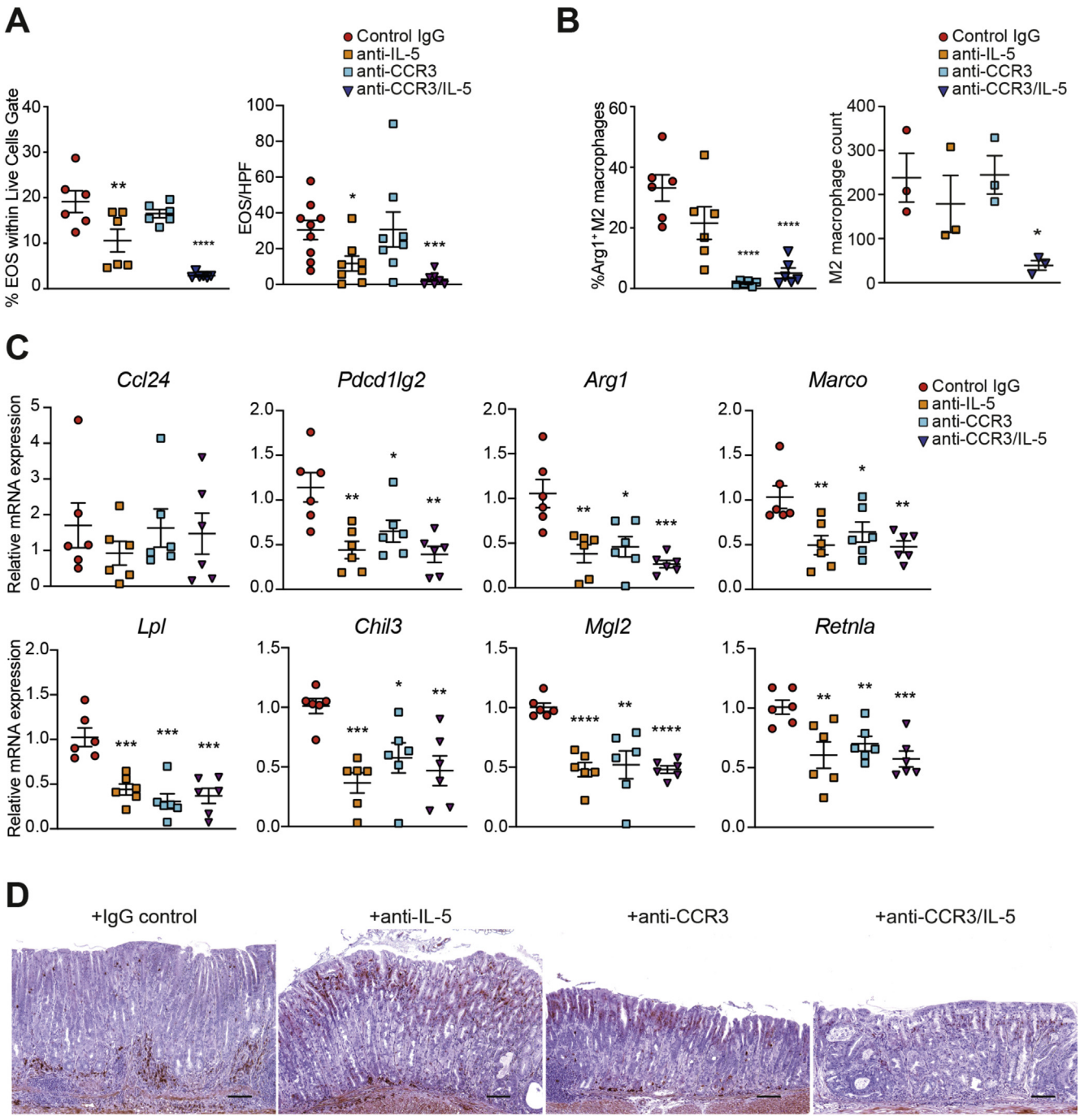

Supplementary Figure 7. Eosinophil (EOS) depletion is effective in decreasing peripheral (BM) and local (gastric) eosinophils, and reduces M2 macrophages and expression of M2-associated genes in SAMP stomachs. (*A*) Frequency of peripheral (BM)-derived eosinophils (*left panel*) and eosinophil count (*right panel*), (*B*) M2 macrophage frequency (*left panel*), and M2 macrophage count (*right panel*, defined as IL-33^{+}CD163^{+} cells shown in Figure 6*A*, *middle panels*) in SAMP corpus after eosinophil depletion by administration of anti-IL5 and anti-CCR3, alone and in combination, vs IgG-treated controls (N = 4-9). (*C*) Relative transcript levels of M2-associated molecules, normalized by *36B4* and expressed as fold-change vs IgG-treated controls (with mean set arbitrarily as 1) (N = 6). mRNA, messenger RNA. (*D*) Representative immunohistochemistry images localizing IL33 (N = 4). Original magnification ×10+1.25; *scale bars*: 100 μm. *$P < .05$, **$P < .01$, ***$P < .001$, ****$P < .0001$.

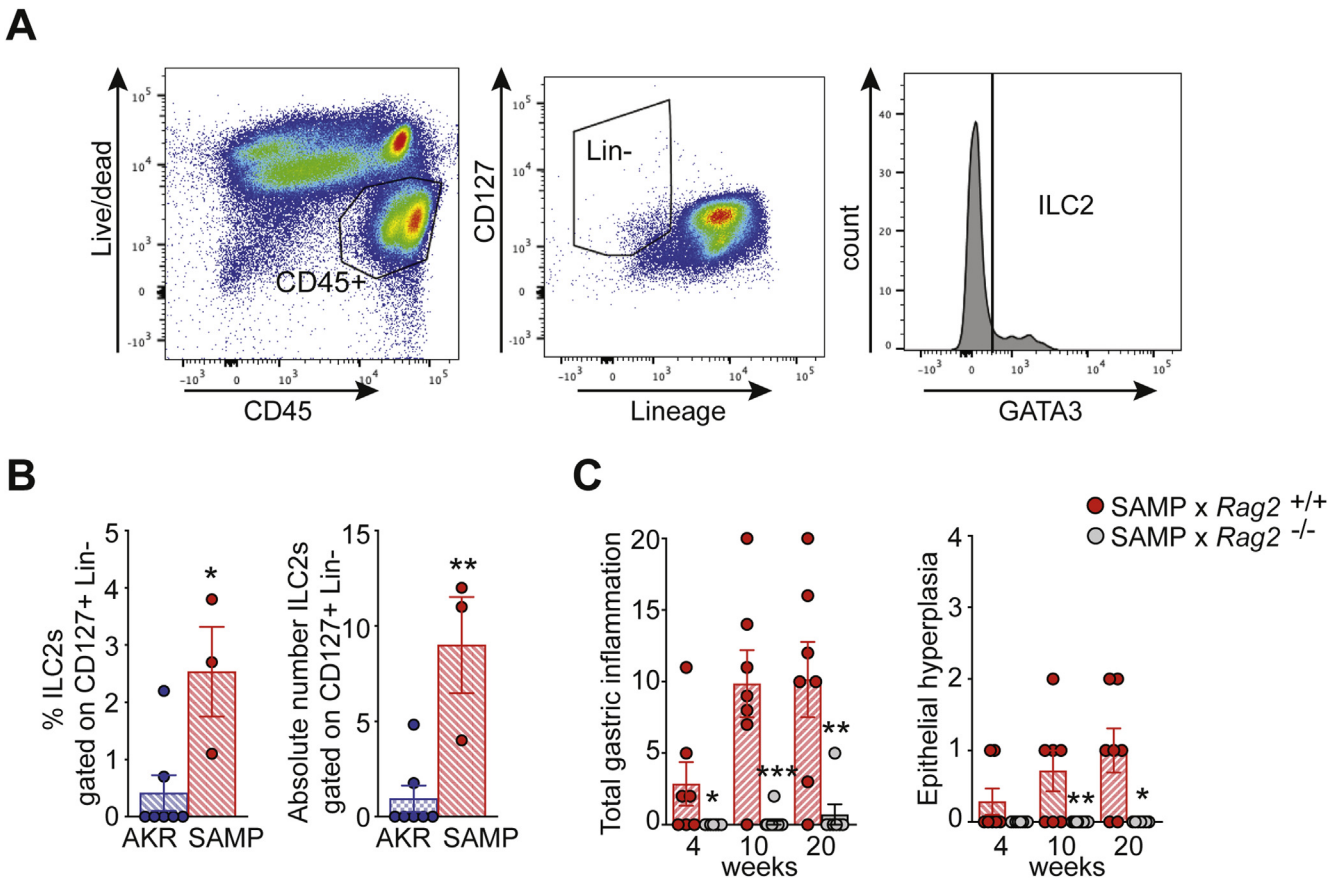

Supplementary Figure 8. Evidence that aberrant adaptive immune responses, and not increased ILC2 frequency, is essential for development of gastritis/SPEM in SAMP mice. Corpus tissues were excised from stomachs of SAMP and AKR and processed into single-cell suspensions for flow cytometric analysis of ILC2s using the following gating strategy: (*A*) live cells were gated on $CD45^{+}$, then on $CD127^{+}$ cells negative for lineage markers CD3 (T cells), CD11c (dendric cells), B220 (B cells), CD11b (myeloid cells), Ly6g, and Ter-119 (granulocytes), and positive for the transcription factor GATA3, (*B*) with ILC2s reported as percentages and absolute numbers (N = 3-7). $^{*}P < .05$, $^{**}P < .01$. (*C*) Total inflammation (*left panel*) and hepithelial hyperplasia (*right panel*) in corpus from SAMP × *Rag2*$^{-/-}$ mice vs wild type controls (N = 7-15). $^{*}P < .05$, $^{**}P < .01$, $^{***}P < .001$.